

ขั้นตอนวิธีเชิงตัวเลขสำหรับปัญหาการไหลผ่านของ
ของไหลอุดมคติที่ยุบตัวไม่ได้



นางเพียงพบ มนต์นวลปรารงค์

วิทยานิพนธ์นี้เป็นส่วนหนึ่งของการศึกษาตามหลักสูตรปริญญาวิทยาศาสตรดุษฎีบัณฑิต

สาขาวิชาคณิตศาสตร์ประยุกต์

มหาวิทยาลัยเทคโนโลยีสุรนารี

ปีการศึกษา 2544

ISBN 974-533-024-8

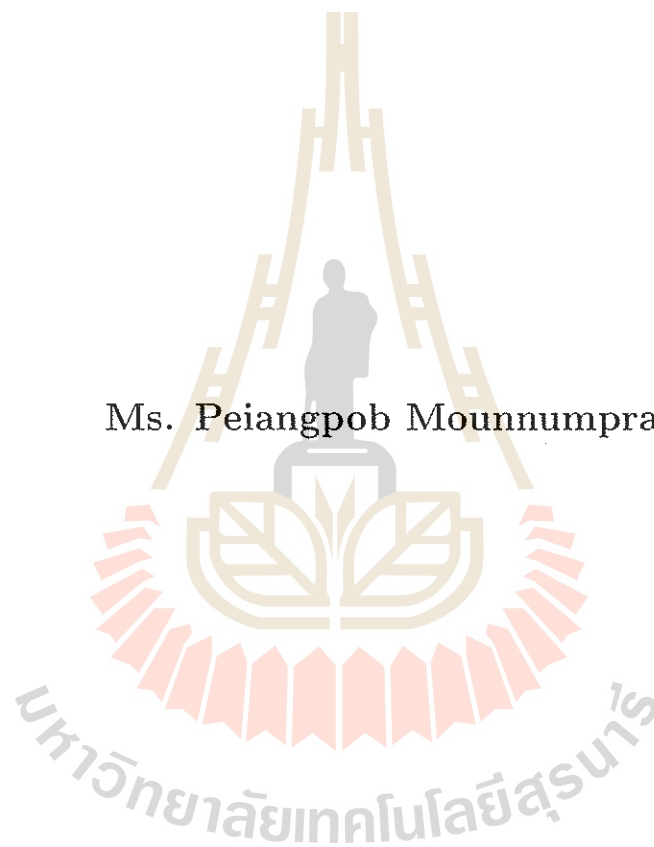


ศูนย์บรรณสารและสื่อการศึกษา

มหาวิทยาลัยเทคโนโลยีสุรนารี

NUMERICAL ALGORITHMS FOR FLOWING-
THROUGH PROBLEM OF AN IDEAL
INCOMPRESSIBLE FLUID

Ms. Peiangpob Mounnumprang



A Thesis Submitted in Partial Fulfillment of the Requirements
for the Degree of Doctor of Philosophy in Applied Mathematics
Suranaree University of Technology
Academic Year 2001
ISBN 974-533-024-8

NUMERICAL ALGORITHMS FOR FLOWING-THROUGH PROBLEM
OF AN IDEAL INCOMPRESSIBLE FLUID

THESIS ADVISOR: ASSOC. PROF. DR. NIKOLAY MOSHKIN, Ph.D.
115 PP. ISBN 974-533-024-8

NUMERICAL ALGORITHM / FLOWING-THROUGH / IDEAL / INCOM-
PRESSIBLE FLUID / IMPERMEABLE / FINITE-DIFFERENCE / EULER
EQUATIONS / VORTICITY

This thesis is involved with a numerical method for an ideal incompressible fluid flow through a bounded domain with inflow, outflow and impermeable parts of the boundary. The finite-difference scheme is used to solve the Euler equations for certain geometries of flow domain and boundary conditions. The numerical algorithms can be useful in predicting flows for three different kinds of boundary conditions on inflow and outflow parts of the channel boundary.

In the first case it is given the tangent components of vorticity and normal component of the velocity vector on the inflow parts of domain boundary and only the normal component of the velocity vector on the outflow parts of channel boundary.

In the second case is given the whole vector of the velocity on inflow parts of domain boundaries and only the normal component of the velocity vector on the outflow parts of channel boundary.

In the third case the boundary condition on the inflow parts of the domain boundary is the same as in the second case and on the outflow parts only the pressure is given.

School of Mathematics

Academic Year 2001

Student  _____

Advisor _____

Acknowledgements

I would like to express my sincere gratitude to my advisor Assoc. Prof. Dr. Nikolay P. Moshkin, School of Mathematics, Institute of Science, Suranaree University of Technology for his kind guidance and support throughout the course of this research. I have been working under his invaluable supervision for about five years and have had many unique research experiences which I will cherish throughout my life.

I am also very grateful to and would like to thank the Chairman of the School of Mathematics of Suranaree University of Technology, Assoc. Prof. Dr. Prapasri Asawakun and all the lecturers who taught and helped me during my study in Suranaree University of Technology. They are Assoc. Prof. Dr. Suwan Tangmanee, Assoc. Prof. Dr. Pairote Sattayatham, Prof. Dr. Sergey V. Meleshko, Assoc. Prof. Dr. B.I. Kvasov, Asst. Prof. Dr. Eckart Schulz and Asst. Prof. Dr. Arjuna Chaiyasena for their help, advice and support.

I want to express my appreciation to Anirut Laudsong, Paladorn Suwanapho, Apichai Hematulin, Asst. Prof. Supot Witayangkurn, Jessada Tantanut, Dr. Wei Wei, Mana Kaomek and Anusorn Ruchirabha for their invaluable professional guidance and friendly encouragement.

In addition, I wish to express my special thanks to Rajabhat Institute Petchburiwittayalongkorn and Government of France for offering the scholarship which enabled me to continue my advanced studies in Suranaree University of Technology, Thailand.

Peiangpob Mounnumprang

Contents

	Page
Abstract in Thai	I
Abstract in English	II
Acknowledgements	III
Contents	IV
List of Tables	VI
List of Figures	VII
Chapter	
I Introduction	1
1.1 Purpose and Background of the Research	1
1.2 General Considerations on the Euler Equations	2
1.2.1 The Equation of Motion of an Ideal Incompressible Fluid	2
1.2.2 Vorticity and Stream Function	3
1.2.3 Conservation Laws	5
1.2.4 Potential and Irrotational Flows	7
1.2.5 Historical Comments	8
1.2.6 Existence and Uniqueness of the Solution	9
1.2.7 Comment (Existence and Uniqueness)	9
1.3 Mathematical Formulation of Flowing-Through Problems . .	10
1.4 Review of Literatures	12
1.4.1 Theoretical Investigation of Initial Boundary Value	
Problems for Euler Equations	12
1.4.2 Analyzing Numerical Schemes	13
1.5 Survey of the Thesis	14
II Numerical Methods for Steady Flowing-Through Problems:	
Problem 2 and Problem 3	16
2.1 Introduction	16
2.2 Mathematical Formulation	16
2.2.1 The Euler Equations in Terms of New Unknown Func-	
tion $w(x, y)$ and $q(x, y)$	18

Contents (Continued)

Chapter	Page
2.2.2	Transformation from Cartesian Coordinates (x, y) to Generalized Curvilinear Coordinates (φ, ψ) 21
2.2.3	The Equations in New Generalized Curvilinear Coordinates (φ, ψ) 24
2.3	Discretization of the Equations and the Solution Procedure . 32
2.3.1	The Method of Block SOR 38
2.3.2	The Method of Stabilizing Corrections 40
2.3.3	Interpretation and Presentation of Results of Numerical Calculations 40
2.4	Results and Discussions 44
2.4.1	90 Degree Elbow with Contraction 44
2.4.2	Convergence of Numerical Algorithm 45
2.4.3	Numerical Results for 90 Degree Elbow with Contraction 49
2.4.4	Numerical Results for Two-Dimensional Channel with Curved Walls 58
2.4.5	Numerical Results for α Degree Elbow 73
2.5	Conclusions 75
III	Numerical Methods for Steady Flowing-Through Problem:
	Problem 1 80
3.1	Introduction 80
3.2	Mathematical Statement of the Problem 80
3.3	Problem in Two-Dimensional Generalized Curvilinear Coordinates 81
3.4	Relations between Metric and Differential Equations 82
3.5	Discretization of the Equations and the Solution Procedure . 85
3.6	Convergence, Results and Discussions 89
3.6.1	Euler Equations with Exact Solution 89
3.6.2	Flow Through a Channel with Curved Walls 94
3.7	Conclusions 111
IV	Conclusions 112
	References 115
	Appendix
A.	Examples of MAPLE Program. 120
	Curriculum Vitae 126

List of Tables

Table		Page
2.1	Convergence to exact solution. The results of numerical simulations for different grids for 90 degree elbow.	46
2.2	Rate of convergence of numerical algorithm.	47
2.3	The choice of the relaxation parameter. The results of numerical calculations for the case of 90 degree elbow with $x_0 = 2.0$, $y_0 = 2.0$, $R_1 = 1.0$, $R_2 = 2.0$, $\frac{R_2 - R_1}{R_2} = \frac{1}{2}$	48
2.4	Detailed description of data of numerical simulations for 90 degree elbow with contraction. Tolerance criteria $\epsilon_\phi = 10^{-4}$, $\epsilon_w = 10^{-4}$, $\epsilon_q = 10^{-4}$	49
2.5	The maximum of $ \varphi_{C'D'}(\psi) $ for different length of exit for 90 degree elbow with contraction, $y_0 = 2$, $R_1 = 1$, $R_2 = 2$	57
2.6	Results of numerical simulations for different grids.	59
2.7	Choices of the relaxation parameter for channel with curved walls $x_{1t} = 1.0$, $x_{2t} = 2.0$, $x_{Lt} = 5.0$, $h_t = 0.0$, $x_{1d} = 2.0$, $x_{2d} = 3.0$, $x_{Ld} = 5.0$, $h_d = 0.05$	60
2.8	Detailed description of results of numerical simulations with tolerances criteria $\epsilon_\phi = 10^{-4}$, $\epsilon_w = 10^{-4}$, $\epsilon_q = 10^{-4}$. Channel with curve walls.	61
2.9	Detailed descriptions of numerical experiments on different grids for α degree elbow with $L_{x0} = 2.0$, $y_0 = 2.0$, $R_1 = 1.0$, $R_2 = 2.0$	74
3.1	Absolute errors of stream function and vorticity and rate of convergence for test problem (3.6.5).	92
3.2	Absolute errors of stream function and vorticity and rate of convergence for test problem (3.6.9).	92
3.3	Computed error parameters, sensitivity.	97

List of Figures

Figure	Page
1.1 Evolving in time of closed curve.	6
1.2 Normal vector on surface.	7
1.3	8
1.4 Sketch of a domain.	11
2.1 Sketch of a physical domain.	17
2.2 Physical and computational domain.	21
2.3 Domain $A'B'C'D'$ for problem 3'.	30
2.4 Domain $A'B'C'D'$ for problem 2'.	31
2.5 Sketch of finite difference grid.	34
2.6 Flowchart of the iterative process.	38
2.7 Computational stencil for finite difference equation (2.3.5).	39
2.8 Sketch of an elbow-shaped domain and coordinates.	45
2.9 Pressure contours for 90 degree elbow with contraction, $\frac{R_2-R_1}{R_2} = \frac{2}{3}$	51
2.10 Pressure contours for 90 degree elbow with contraction, $\frac{R_2-R_1}{R_2} = \frac{1}{2}$	51
2.11 Pressure contours for 90 degree elbow with contraction, $\frac{R_2-R_1}{R_2} = \frac{1}{3}$	52
2.12 Pressure contours for 90 degree elbow with contraction, $\frac{R_2-R_1}{R_2} = \frac{1}{3}$	52
2.13 Colored graphics of pressure contours for 90 degree elbow with contraction, $\frac{R_2-R_1}{R_2} = \frac{2}{3}$	53
2.14 Colored graphics of pressure contours for 90 degree elbow with contraction, $\frac{R_2-R_1}{R_2} = \frac{1}{2}$	53
2.15 Colored graphics of pressure contours for 90 degree elbow with contraction, $\frac{R_2-R_1}{R_2} = \frac{1}{3}$	54
2.16 Colored graphics of pressure contours for 90 degree elbow with contraction, $\frac{R_2-R_1}{R_2} = \frac{1}{3}$	54
2.17 Velocity vectors for 90 degree elbow with contraction, $\frac{R_2-R_1}{R_2} = \frac{2}{3}$	55
2.18 Streamlines for 90 degree elbow with contraction, $\frac{R_2-R_1}{R_2} = \frac{2}{3}$	55
2.19 Pressure as a function of φ along streamlines $\psi = -1, -0.5, 0$ for 90 degree elbow with contraction, $\frac{R_2-R_1}{R_2} = \frac{2}{3}, R_1 = 1, R_2 = 3, x_0 = 2, y_0 = 2, P_{CD} = 2$	56
2.20 Modulus of the velocity vector as a function of φ along streamline $\psi = -1, -0.5, 0$ for 90 degree elbow with contraction, $\frac{R_2-R_1}{R_2} = \frac{2}{3}, R_1 = 1, R_2 = 3, x_0 = 2, y_0 = 2, P_{CD} = 2$	56
2.21 Graph of $C'D'$ boundary for 90 degree elbow with contraction, $\frac{R_2-R_1}{R_2} = \frac{2}{3}, R_1 = 1, R_2 = 3, x_0 = 2, y_0 = 2, P_{CD} = 2$	57

List of Figures (Continued)

Figure	Page
2.22 Physical domain.	58
2.23 Pressure contours by T. W. Roberts et al. Contour increment $\Delta P = 0.01$	62
2.24 Pressure contours for channel with curved walls. Results of numerical simulations for $x_{1d} = 1$, $x_{2d} = 2$, $x_{Ld} = 3$, $h_d = 0.05$, $N1 = 97$, $N2 = 33$. Contour increment $\Delta P = 0.01$	62
2.25 Pressure contours for channel with curved walls. Results of numerical simulations for $x_{1t} = 0$, $x_{2t} = 0$, $x_{Lt} = 3$, $h_t = 0$, $x_{1d} = 1$, $x_{2d} = 2$, $x_{Ld} = 3$, $h_d = 0.04$, $N1 = 41$, $N2 = 41$	63
2.26 Pressure contours for channel with curved walls. Results of numerical simulations for $x_{1t} = 0$, $x_{2t} = 0$, $x_{Lt} = 3$, $h_t = 0$, $x_{1d} = 1$, $x_{2d} = 2$, $x_{Ld} = 3$, $h_d = 0.1$, $N1 = 41$, $N2 = 41$	63
2.27 Pressure contours for channel with curved walls. Results of numerical simulations for $x_{1t} = 0$, $x_{2t} = 0$, $x_{Lt} = 3$, $h_t = 0$, $x_{1d} = 1$, $x_{2d} = 2$, $x_{Ld} = 3$, $h_d = -0.07$, $N1 = 41$, $N2 = 41$	64
2.28 Pressure contours for channel with curved walls. Results of numerical simulations for $x_{1t} = 0$, $x_{2t} = 0$, $x_{Lt} = 3$, $h_t = 0$, $x_{1d} = 1.5$, $x_{2d} = 2.5$, $x_{Ld} = 3$, $h_d = -0.03$, $N1 = 41$, $N2 = 41$	64
2.29 Pressure contours for channel with curved walls. Results of numerical simulations for $x_{1t} = 2$, $x_{2t} = 3$, $x_{Lt} = 5$, $h_t = -0.1$, $x_{1d} = 2$, $x_{2d} = 3$, $x_{Ld} = 5$, $h_d = 0.1$, $N1 = 41$, $N2 = 41$	65
2.30 Pressure contours for channel with curved walls. Results of numerical simulations for $x_{1t} = 2$, $x_{2t} = 3$, $x_{Lt} = 5$, $h_t = -0.1$, $x_{1d} = 2.5$, $x_{2d} = 3.5$, $x_{Ld} = 5$, $h_d = 0.1$, $N1 = 41$, $N2 = 41$	65
2.31 Pressure contours for channel with curved walls. Results of numerical simulations for $x_{1t} = 1$, $x_{2t} = 2$, $x_{Lt} = 5$, $h_t = -0.03$, $x_{1d} = 2$, $x_{2d} = 3$, $x_{Ld} = 5$, $h_d = 0.03$, $N1 = 61$, $N2 = 61$	66
2.32 Pressure contours for channel with curved walls. Results of numerical simulations for $x_{1t} = 1$, $x_{2t} = 2$, $x_{Lt} = 5$, $h_t = -0.1$, $x_{1d} = 3$, $x_{2d} = 4$, $x_{Ld} = 5$, $h_d = 0.1$, $N1 = 41$, $N2 = 41$	66
2.33 Pressure contours for channel with curved walls. Results of numerical simulations for $x_{1t} = 2$, $x_{2t} = 3$, $x_{Lt} = 5$, $h_t = 0.2$, $x_{1d} = 2$, $x_{2d} = 3$, $x_{Ld} = 5$, $h_d = -0.2$, $N1 = 61$, $N2 = 61$	67
2.34 Pressure contours for channel with curved walls. Results of numerical simulations for $x_{1t} = 2$, $x_{2t} = 3$, $x_{Lt} = 5$, $h_t = 0.1$, $x_{1d} = 2$, $x_{2d} = 3$, $x_{Ld} = 5$, $h_d = -0.1$, $N1 = 41$, $N2 = 41$	67
2.35 Pressure contours for channel with curved walls. Results of numerical simulations for $x_{1t} = 2$, $x_{2t} = 3$, $x_{Lt} = 5$, $h_t = 0.05$, $x_{1d} = 2.5$, $x_{2d} = 3.5$, $x_{Ld} = 5$, $h_d = -0.05$, $N1 = 41$, $N2 = 41$	68

List of Figures (Continued)

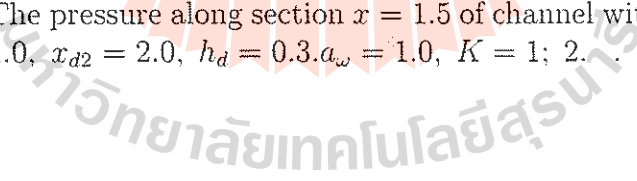
Figure	Page
2.36 Pressure contours for channel with curved walls. Results of numerical simulations for $x_{1t} = 2$, $x_{2t} = 3$, $x_{Lt} = 5$, $h_t = 0.05$, $x_{1d} = 3$, $x_{2d} = 4$, $x_{Ld} = 5$, $h_d = -0.05$, $N_1 = 41$, $N_2 = 41$	68
2.37 Pressure contours for channel with curved walls. Results of numerical simulations for $x_{1t} = 2$, $x_{2t} = 3$, $x_{Lt} = 5$, $h_t = -0.1$, $x_{1d} = 2$, $x_{2d} = 3$, $x_{Ld} = 5$, $h_d = -0.1$, $N_1 = 41$, $N_2 = 41$	69
2.38 Pressure contours for channel with curved walls. Results of numerical simulations for $x_{1t} = 2$, $x_{2t} = 3$, $x_{Lt} = 5$, $h_t = -0.1$, $x_{1d} = 2.5$, $x_{2d} = 3.5$, $x_{Ld} = 5$, $h_d = -0.1$, $N_1 = 41$, $N_2 = 41$	69
2.39 Streamlines for channel with curved walls. Results of numerical simulations for $x_{1t} = 1$, $x_{2t} = 2$, $x_{Lt} = 5$, $h_t = -0.1$, $x_{1d} = 2$, $x_{2d} = 3$, $x_{Ld} = 5$, $h_d = 0.1$, $N_1 = 21$, $N_2 = 21$	70
2.40 Streamlines for channel with curved walls. Results of numerical simulations for $x_{1t} = 2$, $x_{2t} = 3$, $x_{Lt} = 5$, $h_t = 0.2$, $x_{1d} = 2$, $x_{2d} = 3$, $x_{Ld} = 5$, $h_d = -0.2$, $N_1 = 21$, $N_2 = 21$	70
2.41 Velocity vectors for channel with curved walls. Results of numerical simulations for $x_{1t} = 1$, $x_{2t} = 2$, $x_{Lt} = 5$, $h_t = -0.1$, $x_{1d} = 2$, $x_{2d} = 3$, $x_{Ld} = 5$, $h_d = 0.1$, $N_1 = 21$, $N_2 = 21$	71
2.42 Velocity vectors for channel with curved walls. Results of numerical simulations for $x_{1t} = 2$, $x_{2t} = 3$, $x_{Lt} = 5$, $h_t = 0.2$, $x_{1d} = 2$, $x_{2d} = 3$, $x_{Ld} = 5$, $h_d = -0.2$, $N_1 = 21$, $N_2 = 21$	71
2.43 Colored graphics of pressure contours for channel with curved walls. Results of numerical simulations for $x_{1t} = 1$, $x_{2t} = 2$, $x_{Lt} = 5$, $h_t = -0.1$, $x_{1d} = 2$, $x_{2d} = 3$, $x_{Ld} = 5$, $h_d = 0.1$, $N_1 = 61$, $N_2 = 61$	72
2.44 Colored graphics of pressure contours for channel with curved walls. Results of numerical simulations for $x_{1t} = 2$, $x_{2t} = 3$, $x_{Lt} = 5$, $h_t = 0.2$, $x_{1d} = 2$, $x_{2d} = 3$, $x_{Ld} = 5$, $h_d = -0.2$, $N_1 = 61$, $N_2 = 61$	72
2.45 Geometry of α° elbow channel.	73
2.46 Pressure contours for channel with curved walls. Results of numerical simulations for $R_1 = 1$, $R_2 = 2$, $L_{x0} = 2$, $y_0 = 2$, $\alpha = \pi/2$, $N_1 = 41$, $N_2 = 41$	76
2.47 Pressure contours for channel with curved walls. Results of numerical simulations for $R_1 = 1$, $R_2 = 2$, $L_{x0} = 2$, $y_0 = 2$, $\alpha = 3\pi/4$, $N_1 = 21$, $N_2 = 21$	76
2.48 Pressure contours for channel with curved walls. Results of numerical simulations for $R_1 = 1$, $R_2 = 2$, $L_{x0} = 2$, $y_0 = 2$, $\alpha = \pi$, $N_1 = 21$, $N_2 = 21$	77

List of Figures (Continued)

Figure	Page
2.49 Pressure contours for channel with curved walls. Results of numerical simulations for $R_1 = 1$, $R_2 = 2$, $L_{x0} = 2$, $y_0 = 2$, $\alpha = 5\pi/4$, $N_1 = 21$, $N_2 = 21$	77
2.50 Colored graphics of pressure contours for channel with curved walls. Results of numerical simulations for $R_1 = 1$, $R_2 = 2$, $L_{x0} = 2$, $y_0 = 2$, $\alpha = \pi/2$, $N_1 = 41$, $N_2 = 41$	78
2.51 Colored graphics of pressure contours for channel with curved walls. Results of numerical simulations for $R_1 = 1$, $R_2 = 2$, $L_{x0} = 2$, $y_0 = 2$, $\alpha = 3\pi/4$, $N_1 = 21$, $N_2 = 21$	78
2.52 Colored graphics of pressure contours for channel with curved walls. Results of numerical simulations for $R_1 = 1$, $R_2 = 2$, $L_{x0} = 2$, $y_0 = 2$, $\alpha = \pi$, $N_1 = 21$, $N_2 = 21$	79
2.53 Colored graphics of pressure contours for channel with curved walls. Results of numerical simulations for $R_1 = 1$, $R_2 = 2$, $L_{x0} = 2$, $y_0 = 2$, $\alpha = 5\pi/4$, $N_1 = 21$, $N_2 = 21$	79
3.1 Physical and computational domain.	82
3.2 Computational domain.	86
3.3 Stencil of the finite-difference equation for ω	88
3.4 Flow domain of the test problem.	90
3.5 Pressure contours for solution (3.6.5)	93
3.6 Pressure contours for solution (3.6.9)	93
3.7 Pressure along lower boundary for solution (3.6.5)	93
3.8 Pressure along lower boundary for solution (3.6.9)	93
3.9 Pressure along section $x = 0.25$ for solution (3.6.5)	93
3.10 Pressure along section $x = 0.25$ for solution (3.6.9)	93
3.11 Sketch of channel with curved walls.	95
3.12 Pressure at line $x = 1.5$. Numerical solutions computed on four grids with $h_1 = 1/20$, $h_2 = h_1/2$, $h_3 = h_1/4$, $h_4 = h_1/8$	98
3.13 Pressure contours for $a_\omega = 0$, $K = 1$	101
3.14 Pressure contours for $a_\omega = 0.1$, $K = 1$	101
3.15 Pressure contours for $a_\omega = 1.0$, $K = 1$	101
3.16 Pressure contours for $a_\omega = 1.0$, $K = 2$	102
3.17 Pressure contours for $a_\omega = 5.0$, $K = 1$	102
3.18 Pressure contours for $a_\omega = 5.0$, $K = 2$	102
3.19 Isolines $\psi = \text{constant}$ for the values of the levels vary from 0 to 1.0 with interval 0.0625. $a_\omega = 5.0$, $K = 1$	103
3.20 Isolines $\psi = \text{constant}$ for the values of the levels vary from 0 to 1.0 with interval 0.0625. $a_\omega = 5.0$, $K = 2$	103

List of Figures (Continued)

Figure	Page
3.21 The pressure along lower boundary of channel with $x_d = 3.0$, $x_{d1} = 1.0$, $x_{d2} = 2.0$, $h_d = 0.05$. $a_w = 0.0; 0.1; 1.0$; $K = 1$	104
3.22 The pressure along lower boundary of channel with $x_d = 3.0$. $x_{d1} = 1.0$, $x_{d2} = 2.0$, $h_d = 0.05$. $a_w = 0.1$; $K = 1; 2$	104
3.23 The pressure along section $x = 1.5$ of channel with $x_d = 3.0$, $x_{d1} = 1.0$, $x_{d2} = 2.0$, $h_d = 0.05$. $a_w = 0.0; 0.1; 1.0$ $K = 1$	105
3.24 The pressure along section $x = 1.5$ of channel with $x_d = 3.0$, $x_{d1} = 1.0$, $x_{d2} = 2.0$, $h_d = 0.05$. $a_w = 1.0$ $K = 1; 2$	105
3.25 Pressure contours for $a_w = 0.0$, $K = 1$	106
3.26 Pressure contours for $a_w = 0.1$, $K = 1$	106
3.27 Pressure contours for $a_w = 1.0$, $K = 1$	106
3.28 Pressure contours for $a_w = 1.0$, $K = 2$	107
3.29 Pressure contours for $a_w = 5.0$, $K = 1$	107
3.30 Pressure contours for $a_w = 5.0$, $K = 2$	107
3.31 Isolines $\psi = \text{constant}$ for the values of the levels vary from 0 to 1.0 with interval 0.0625. $a_w = 5.0$, $K = 1$	108
3.32 Isolines $\psi = \text{constant}$ for the values of the levels vary from 0 to 1.0 with interval 0.0625. $a_w = 5.0$. $K = 2$	108
3.33 The pressure along lower boundary of channel with $x_d = 3.0$. $x_{d1} = 1.0$, $x_{d2} = 2.0$, $h_d = 0.3$. $a_w = 0; 0.1; 1.0$; $K = 1$	109
3.34 The pressure along lower boundary of channel with $x_d = 3.0$, $x_{d1} = 1.0$, $x_{d2} = 2.0$, $h_d = 0.3$. $a_w = 1.0$; $K = 1; 2$	109
3.35 The pressure along section $x = 1.5$ of channel with $x_d = 3.0$. $x_{d1} = 1.0$, $x_{d2} = 2.0$, $h_d = 0.3$. $a_w = 0; 0.1; 1.0$, $K = 1$	110
3.36 The pressure along section $x = 1.5$ of channel with $x_d = 3.0$. $x_{d1} = 1.0$, $x_{d2} = 2.0$, $h_d = 0.3$. $a_w = 1.0$, $K = 1; 2$	110



Chapter I

Introduction

1.1 Purpose and Background of the Research

One of the main problems of fluid dynamics is the motion of fluid in a given domain whose boundaries do not only consist of solid impermeable parts but also the inflow and outflow parts. We will call such kind of problem as the “flowing-through” problem.

Many flow properties can be described by the inviscid approximation (for example, determination of the pressure distribution). The inviscid flows in which the viscosity forces can be neglected play an important role in fluid mechanics. In many cases, the hypothesis of incompressibility is a good approach of the real process in gas. The Euler equations for an incompressible ideal fluid are a classical model of hydrodynamics. The Euler equations can be interpreted as the limit of the Navier-Stokes equations of vanishing viscosity, and their character is hyperbolic in the unsteady cases.

The purpose of this thesis is to develop a numerical method for the Euler equations of an ideal homogeneous incompressible fluid flows when the boundary of the domain includes the inflow, the outflow and the impermeable parts as well.

Theoretical investigation of initial boundary value problems for the Euler equations was initiated by N. M. Gunter (1927) and L. Lichtenstein (1929). These authors obtained basic results for the cases when the liquid filled the whole space, or a container with impermeable walls, and when the vector of mass forces was potential. However, the demonstration that the boundary value problem for the Euler equations of an ideal fluid is well-posed, is quite difficult even for the problem considered in small time intervals. The results obtained in this field are mostly local in time. It was N. E. Kochin (1956) who first studied the flowing-through problem in a model formulation, in which the boundary conditions at the entrance were formulated for a velocity vortex. The two-dimensional non-stationary problem with a given vortex at the inlet part was studied by V. I. Yudovich (1964). A. V. Kazhikhov *et al.* (1980) proved the short time existence results for non-stationary problem of an ideal liquid flow through a bounded domain, in case the total vector of velocity is given on the inflow parts of the boundary, while its normal component is given on the outflow parts of the boundary.

The numerical methods for the solution of the Euler equations of an ideal

incompressible fluid flow through a bounded domain with the inflow and outflow parts of boundaries have not yet been considered in detail. The goal of this thesis is to study the numerical methods for approximating solutions of such flowing-through problems.

1.2 General Considerations on the Euler Equations

This section has an introductory nature, wherein we discuss the fundamental equations describing the motion of an incompressible nonviscous fluid and formulate some elementary properties.

1.2.1 The Equation of Motion of an Ideal Incompressible Fluid

Fluid mechanics does not study the dynamics of the individual molecules constituting the fluid. We want to investigate the gross behavior of many of molecules. For this purpose, we assume the fluid as a continuum, a point of which is a very small portion of the real fluid. This small volume, a point in our mathematical description, will be called *fluid particle* or element of fluid.

Let D be a region in two- or three- dimensional space filled with a fluid. Let $\mathbf{X} = (X^1, X^2, X^3)$, $\mathbf{X} \in D$ be a coordinates of fluid particle at time $t = 0$. Let $\mathbf{x} = (x^1, x^2, x^3)$, $\mathbf{x} \in D$ be a coordinates of the some fluid particle at time t . Then an incompressible motion is, by definition, a function

$$\mathbf{x} = \varphi(\mathbf{X}, t) \quad (\text{or } x^i = \varphi^i(\mathbf{X}, t)) \quad (1.2.1)$$

such that:

- a) φ is invertible;
- b) φ and φ^{-1} are smooth enough so that the main operations of calculus may be performed on them;
- c) $\mathbf{X} = \varphi(\mathbf{X}, 0)$, $\varphi(\mathbf{X}, t_1 + t_2) = \varphi(\varphi(\mathbf{X}, t_1), t_2)$.

If \mathbf{X} is fixed and t is changed, then equation (1.2.1) determines a *trajectory* of fluid particle P which initially placed at point \mathbf{X} . From another side, If t is fixed, then equation (1.2.1) determines the transformation of the fluid domain at time $t = 0$ to the fluid domain at time $t = t_1$.

In spite of the fact that (1.2.1) determines the fluid motion, it is also important to study the time evolution at given point $\mathbf{x} \in D$ of the density field $\rho(\mathbf{x}, t)$, velocity field $\mathbf{u} = \mathbf{u}(\mathbf{x}, t)$ and so on.

The derivation of the fluid motion equations is based on three basic principles:

- I: mass is neither created or destroyed.
- II: the rate of change of momentum of a portion of the fluid equals the force applied to it (*Newton's second law*),
- III: energy is neither created nor destroyed.

By the law of conservation of mass together with the condition of incompressibility, we have

$$\operatorname{div} \mathbf{u}(\mathbf{x}, t) \equiv \nabla \cdot \mathbf{u}(\mathbf{x}, t) = 0, \quad \forall \mathbf{x} \in D, t \in \mathbb{R}. \quad (1.2.2)$$

Equation (1.2.2) is called the *continuity equation* for incompressible flows.

Let us define an *ideal fluid* as one with the following property: for any motion of the fluid, there is a function $P(\mathbf{x}, t)$ called the *pressure* such that if S is a surface in the fluid with a chosen unit normal \mathbf{n} , the force of stress exerted across the surface S per unit area at $\mathbf{x} \in S$ at time t is $P(\mathbf{x}, t) \cdot \mathbf{n}$. By Newton's second law (force = mass \otimes acceleration), we got the differential equation of the law of balance of momentum.

$$\rho \left(\frac{\partial \mathbf{u}}{\partial t} + (\mathbf{u} \cdot \nabla) \mathbf{u} \right) = -\nabla P + \rho \mathbf{f} \quad (1.2.3)$$

where $\mathbf{f} = \mathbf{f}(\mathbf{x}, t)$ is external force per unity volume.

Equation (1.2.3), together with the equation (1.2.2) form the *Euler equations* for an ideal (or perfect) incompressible fluid.

Remarks:

1. In the present research, we will assume the density to be always constant (for simplicity $\rho \equiv 1$).
2. When \mathbf{f} is a potential force ($\mathbf{f} = -\nabla U$ for some scalar field U), we can modify equation (1.2.3) to

$$\frac{\partial \mathbf{u}}{\partial t} + (\mathbf{u} \cdot \nabla) \mathbf{u} = -\nabla P \quad (1.2.4)$$

with P replaced by $P + U$.

Later on, we will assume the absence of external forces.

1.2.2 Vorticity and Stream Function

There are two different points of view on fluid motion. Fixing time in equation (1.2.1), we have studied the motion of the fluid by following the evolution of a single particle (the Lagrangian point of view). On the contrary, in the Euler equations, the velocity field $\mathbf{u} = \mathbf{u}(\mathbf{x}, t)$ is the unknown quantity. This means that we fixed a point \mathbf{x} and follow the time evolution of the particle that at time t passes through \mathbf{x} (the Eulerian point of view).

The two points of view are related. If we know all the trajectories of the fluid particles, it is possible to find the velocity field by a simple differentiation. More complicated is the inverse problem. In fact, knowing $\mathbf{u} = \mathbf{u}(\mathbf{x}, t)$, we can find the motion of each particle of fluid by solving the initial value problem for ordinary differential equation,

$$\begin{aligned}\frac{d\varphi(\mathbf{x}, t)}{dt} &= \mathbf{u}(\mathbf{x}, t), \\ \varphi(\mathbf{x}, 0) &= \mathbf{X}.\end{aligned}$$

The lines that are tangent in any point to the velocity field, $\mathbf{u} = \mathbf{u}(\mathbf{x})$, are called *streamlines* or *flow lines*. They vary in time and they are constant in time for steady motion. In this case the streamlines coincide with trajectories of the particles.

A fundamental concept of fluid motion analysis is the concept of the *vorticity field* $\boldsymbol{\omega}(\mathbf{x})$. By definition

$$\boldsymbol{\omega} \equiv \text{rot}(\mathbf{u}) = \nabla \times \mathbf{u}. \quad (1.2.5)$$

The vorticity field $\boldsymbol{\omega}(\mathbf{x})$ gives a measure of how the fluid is rotating. The vorticity field is an important tool in studying the behavior of fluids. The Euler equations can be expressed in terms of vorticity. Using the following vector identity

$$\frac{1}{2}\nabla\mathbf{u}^2 = \mathbf{u} \times \text{rot}(\mathbf{u}) + (\mathbf{u} \cdot \nabla)\mathbf{u}, \quad (1.2.6)$$

the Euler equations can be written as

$$\frac{\partial\mathbf{u}}{\partial t} + \frac{1}{2}\nabla\mathbf{u}^2 - \mathbf{u} \times \text{rot}(\mathbf{u}) = -\nabla P.$$

Taking the curl of both sides

$$\frac{\partial\boldsymbol{\omega}}{\partial t} - \text{rot}(\mathbf{u} \times \boldsymbol{\omega}) = 0$$

Since

$$\text{rot}(\mathbf{u} \times \boldsymbol{\omega}) = (\boldsymbol{\omega} \cdot \nabla)\mathbf{u} - \boldsymbol{\omega}(\nabla \cdot \mathbf{u}) - (\mathbf{u} \cdot \nabla)\boldsymbol{\omega} + \mathbf{u}(\nabla \cdot \boldsymbol{\omega}).$$

We finally obtain

$$\frac{\partial\boldsymbol{\omega}}{\partial t} + (\mathbf{u} \cdot \nabla)\boldsymbol{\omega} = (\boldsymbol{\omega} \cdot \nabla)\mathbf{u}. \quad (1.2.7)$$

However, to study the Euler equations in form (1.2.7), it is necessary to reconstruct the velocity field \mathbf{u} from the vorticity. In other words, we have to solve the following equation in unknown quantity \mathbf{u} :

$$\begin{aligned}\text{rot}(\mathbf{u}) &= \boldsymbol{\omega}, \quad \boldsymbol{\omega} \in C(D), \\ \nabla \cdot \mathbf{u} &= 0.\end{aligned}$$

In two dimension (1.2.7) becomes much simpler. Namely, in the presence of a planar symmetry

$$\mathbf{u} = (u_1, u_2, 0), \quad u_i = u_i(x_1, x_2)$$

only the third component of the vorticity $\omega_3 = \omega$ is present and the right-hand side of (1.2.7) vanishes. Therefore, the Euler equations for the vorticity in two dimensions becomes

$$\frac{\partial \omega}{\partial t} + (\mathbf{u} \cdot \nabla) \omega = 0. \quad (1.2.8)$$

Notice that (1.2.8) implies the conservation of the vorticity along the trajectories.

1.2.3 Conservation Laws

The energy conservation is the first conservation law valid for the ideal fluid. The *energy*, defined as

$$E = \frac{1}{2} \int_D \mathbf{u}^2 dx \quad (1.2.9)$$

is conserved during the motion because in mathematical model there is no mechanism of dissipation: the fluid has neither internal friction nor friction with boundaries.

Theorem 1.2.1. *Let $D \subset \mathbb{R}^3$ be a bounded domain and let \mathbf{u} be a solution of the Euler equations with conservative external forces*

$$\frac{\partial \mathbf{u}}{\partial t} + (\mathbf{u} \cdot \nabla) \mathbf{u} = -\nabla(P + U)$$

where $U = U(\mathbf{x}, t)$ is a known function then

$$\frac{d}{dt} E = 0.$$

Remark: The energy conservation law can be extended to unbounded domains. In this case, E is finite if \mathbf{u} decays at infinity fast enough.

For a stationary flow, the energy conservation assumes a very significant form.

Theorem 1.2.2. (Bernoulli) *In an ideal fluid in stationary motion under the action of conservative force with potential U independent of time, the quantity*

$$\varepsilon = \frac{1}{2} \mathbf{u}^2 + (P + U)$$

is constant along the streamlines.

This theorem says that ε remains constant along streamline, but in general varies when we pass from one streamline to another. On the contrary, when the velocity field is irrotational the value of ε does not depend on the choice of the streamline, as follows from:

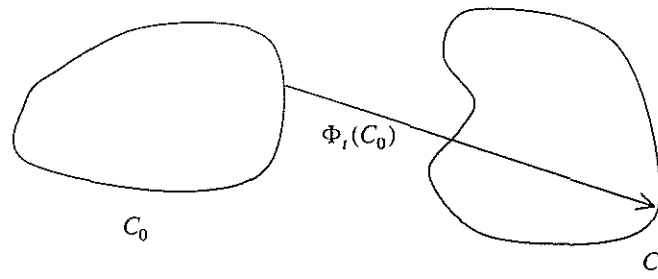


Figure 1.1: Evolving in time of closed curve.

Theorem 1.2.3. (Bernoulli, irrotational flow). Consider an ideal fluid in a stationary irrotational motion in a domain D , under the action of a conservative force with potential U independent of time. Then the quantity

$$\varepsilon = \frac{1}{2} \mathbf{u}^2 + (P + U)$$

is constant.

Remark: The Bernoulli theorems tell us that in the absence of external forces the pressure is greatest when the velocity is smallest and vice-versa. In particular, in a narrowing pipeline the continuity equation implies that, when the pipeline has a smaller section, the velocity must be greater. The Bernoulli theorem ensures that the pressure is smaller.

We proceed now to analyze some conservation laws involving the vorticity. In a fluid motion according to the Euler equations, different layers of the fluid cannot interact between themselves via friction forces. So it is not possible to give rise to or to change the rotation of an ideal fluid. This fact must be reflected in a conservation law involving the vorticity field. This law is expressed by the Kelvin theorem.

Let C_t be a closed curve evolving in time according to the fluid flow (see Figure 1.1)

$$C_t = \phi_t(C_0)$$

We consider the circulation

$$\Gamma(C_t) = \oint_{C_t} \mathbf{u}(t) dl$$

where dl is the infinitesimal element of line in C_t . Then

Theorem 1.2.4. (Kelvin)

$$\frac{d}{dt} \Gamma(C_t) = 0$$

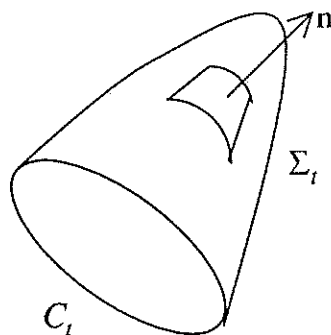


Figure 1.2: Normal vector on surface.

Remark: In terms of the vorticity field the Kelvin theorem has the following consequence: the vorticity flux through a surface Σ_t moving with the fluid

$$\int_{\Sigma_t} \boldsymbol{\omega} \cdot \mathbf{n} d\sigma$$

(\mathbf{n} denotes the normal to surface (Figure. 1.3) remains constant in time. This follows by the Stokes theorem.

1.2.4 Potential and Irrotational Flows

The *irrotational flows* is flows in which the vorticity vanishes every where. A particular example is given by the so-called *potential flows*, those for which there exist a function $\varphi(\mathbf{x}, t)$, such that

$$\mathbf{u}(\mathbf{x}, t) = \nabla\varphi(\mathbf{x}, t). \quad (1.2.10)$$

Clearly any potential flow is also irrotational. (It follows directly by vector identity $\text{rot}(\text{grad } \varphi) \equiv 0$.) The converse is not true: although, it is possible to find, for any irrotational flow, a function φ satisfying (1.2.10), in general, it may be multivalued for a nonsimply connected domain since it can assume many different values depending on the number of loops around the holes.

The interest in studying irrotational divergence-free flows lies in the fact that they are a stationary solution of the Euler equations. To verify this statement, we assume that $\mathbf{u} = \mathbf{u}(t)$ is a solution of the equations

$$\nabla \cdot \mathbf{u} = 0, \quad \text{rot}(\mathbf{u}) = 0 \quad (1.2.11)$$

in a domain $D \subset \mathbb{R}^d$, $d = 2, 3$.

From equation (1.2.6), we know that

$$(\mathbf{u} \cdot \nabla)\mathbf{u} = \frac{1}{2} \nabla \mathbf{u}^2 \quad (1.2.12)$$

and so, for boundary conditions not depending on time, we have a stationary solution of the Euler equations, with the pressure $P = -\frac{1}{2}\mathbf{u}^2$.

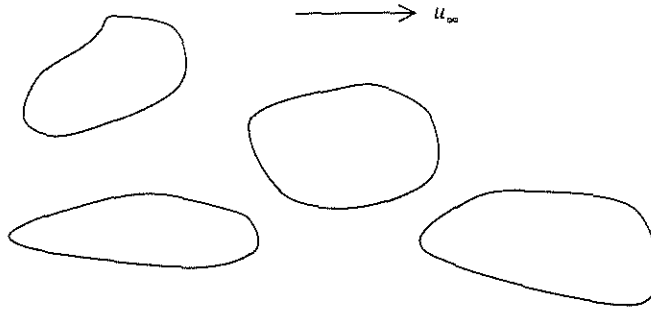


Figure 1.3:

In some problems the boundary conditions depend on time, for instance, when the wall of the region moves with a given law. The Euler equations become (by use (1.2.10) and (1.2.11))

$$\nabla \left(\frac{\partial \varphi}{\partial t} + \frac{1}{2} |\nabla \varphi|^2 + P \right) = 0$$

hence

$$\frac{\partial \varphi}{\partial t} + \frac{1}{2} |\nabla \varphi|^2 + P = \text{constant} \quad (1.2.13)$$

Remark: In bounded, simply connected domain, all the irrotational flows reduce to the trivial one: $\mathbf{u} = 0$.

So in order to have a nontrivial irrotational field, we must consider either nonsimply connected or unbounded domains. Very important in the applications are so-called *external domain*. They are defined as the complement of a finite union of simply connected bounded regions. A domain as in Figure 1.3 has a different topological structure in two and in three dimensions. In fact, it is simply connected in three dimensions and so $\mathbf{u} = \nabla \varphi$ where φ is a harmonic function satisfying the boundary conditions $\frac{\partial \varphi}{\partial \mathbf{u}} = 0$ on ∂D . Specifying the asymptotic behavior

$$\lim_{\|\mathbf{x}\| \rightarrow \infty} \mathbf{u}(\mathbf{x}) = U_{\infty}.$$

We have a unique potential flow (following the uniqueness of the Neumann problem)

In two dimensions, such a domain is not simply connected and the irrotational flows are not necessary potential flows.

1.2.5 Historical Comments

The equations of motion of an ideal fluid were derive by L. Euler (1755). Several mathematicians and physicists, for instance, Bernoulli, d'Alembert, Lagrange, Cauchy, Helmholtz, Kelvin and others, have contributed to further developments of the theory. For a more detail of the deduction and properties of

the Euler equations (not necessary for incompressible flows) consult the classical books in fluid mechanics such as C.K. Batchelor (1970), J. Serrin (1959), A.J. Chorin (1997), L.D. Landau (1968), H. Lamb (1932).

1.2.6 Existence and Uniqueness of the Solution

In this section, we discuss the problem of the existence and uniqueness of the solutions of the Euler equations. The Euler equations are a nonlinear equation. This implies that the construction of its solutions may be a nontrivial task.

The first problem, we meet in the study of a differential equation is to establish an existence and uniqueness theorem for the solutions. This problem is of obvious interest: if a mathematical model of the real world is described by a differential equation, the proof of the existence of a large enough class of solutions is a first verification of the validity of the model. Once the existence of the solutions is ensured, we would like there to be only one solution having a given value at a given instant. If not, the physical state of the system at a time t , could not be uniquely determined by the differential equation itself and the knowledge of the state of the system at a previous time $t_0 < t$. In other words, we would like the Cauchy (initial value) problem associated with our differential equation to be *well-posed*: that is, to have a unique solution with a smooth dependence on the initial data.

Once, we have positively answered these questions about uniqueness and existence, we must develop methodologies and algorithms (implementable numerically if possible) that allow, at least in principle, the approximate calculation of the solution. In the case of the Euler equations, we have satisfactory answers in two dimensions. In three dimensions the theory is much more difficult and it is possible that the solutions may develop singularities in a finite time. Therefore, we confine ourselves to an existence and uniqueness theorem local in time only.

In two dimensions, we are able to construct a solution for any time C. Marchioro (1994). An existence and uniqueness theorem for the solution of the Euler equations in three dimensions for short times was proven, see for instance C. Marchioro (1994).

The shortness of the time in which the solution is constructed depends on the a priori estimates (valid for short times only).

1.2.7 Comment (Existence and Uniqueness)

The solution of the initial value problem associated with the Euler equations, in two dimensions for arbitrary times and in three dimensions for short times has long been known. There is a large literature on the subject. We mention only W. Wolibier (1933), V.I. Yudowich (1963), T. Kato (1972) for two-dimensional existence theorem and D. Ebin (1970), T. Kato (1972), R. Temam (1975), R. Temam (1976), R. Temam (1986), T. Kato (1988) for the three-dimensional case.

1.3 Mathematical Formulation of Flowing-Through Problems

We will present here the three kinds of well-posed boundary value problems for the Euler equations of an ideal incompressible fluid flow through a bounded domain. In our explanation, we follow A. V. Kazhikhov, *et al.* (1980).

Let Ω be a bounded domain in \mathbb{R}^3 whose boundary Γ consists of three parts. Parts of the inflow are denoted by Γ_l^1 . Parts of the outflow are denoted by Γ_m^2 . The part of the impermeable boundary is denoted by Γ^0 . Each component of Γ_α^i is a sufficiently smooth surface. Boundaries Γ_l^1 and Γ_m^2 do not touch each other and the intersection of Γ^0 with Γ_l^1 and Γ_m^2 occurs at a straight angle or a right angle.

Let $\mathbf{x} = (x_1, x_2, x_3)$ denote the Cartesian coordinates of points of Ω , t —the time, $t \in [0, T]$, $\mathbf{u} = (u_1, u_2, u_3)$ —the velocity vector, $\boldsymbol{\omega} = (\omega_1, \omega_2, \omega_3)$ —the vorticity vector, P —the pressure divided by the constant density of the fluid, \mathbf{f} —the vector of mass forces, $Q = \Omega \times (0, T)$, $S^i = \Gamma^i \times (0, T)$, $i = 0, 1, 2$; \mathbf{n} —the unit vector of the outward normal to Γ , and $\boldsymbol{\tau}_2$ and $\boldsymbol{\tau}_3$ linearly independent vectors tangent to Γ^i , $i = 1, 2$.

The motion of a homogeneous ideal incompressible fluid is described by the Euler equations (see, for example, C. K. Batchelor (1979)).

$$\frac{\partial \mathbf{u}}{\partial t} + (\mathbf{u} \cdot \nabla) \mathbf{u} + \nabla P = \mathbf{f}. \quad (1.3.1)$$

$$\nabla \cdot \mathbf{u} = 0, \quad (\mathbf{x}, t) \in Q.$$

At $t = 0$, the velocity field is given by

$$\mathbf{u}|_{t=0} = \mathbf{u}^0(x), \quad (1.3.2)$$

$$\nabla \cdot \mathbf{u}^0 = 0, \quad \mathbf{x} \in \Omega.$$

A typical boundary condition on the solid parts is imposed by prescribing the value of the normal component of velocity vector as

$$(\mathbf{u} \cdot \mathbf{n}) = 0, \quad (\mathbf{x}, t) \in S^0. \quad (1.3.3)$$

and we assume that on the inflow parts of the boundary Γ_l^1 , the normal component of the velocity is given as well,

$$(\mathbf{u} \cdot \mathbf{n}) = g_1 < 0, \quad (\mathbf{x}, t) \in S^1. \quad (1.3.4)$$

Additional boundary conditions must be imposed at the inflow and the outflow parts of the boundary in order to have a well-posed problem. These boundary conditions may vary. We will name the three different kinds of boundary value problems to be considered in this thesis as problem 1, problem 2 and problem 3.

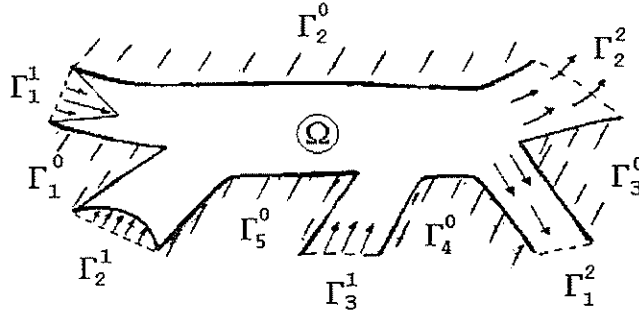


Figure 1.4: Sketch of a domain.

Problem 1:

The additional boundary conditions are the following :

Two tangent components of the vorticity vector are given on the inflow parts of the boundary S_l^1 and the normal component of the velocity vector is given on the outflow parts of the boundary S_m^2 . The whole formulation for problem 1 is therefore as follows:

Find a solution of equation (1.3.1) in the domain Q with initial conditions (1.3.2) and the following boundary conditions

$$\begin{aligned}
 S^0 : \quad & (\mathbf{u} \cdot \mathbf{n}) = 0, \quad (\mathbf{x}, t) \in S^0. \\
 S_l^1 : \quad & (\mathbf{u} \cdot \mathbf{n}) = g_1 < 0, \quad (\boldsymbol{\omega} \cdot \boldsymbol{\tau}_i) = h_i, \quad i = 2, 3, \quad (\mathbf{x}, t) \in S_l^1, \quad l = 1, 2, \dots \\
 S_m^2 : \quad & (\mathbf{u} \cdot \mathbf{n}) = l > 0, \quad (\mathbf{x}, t) \in S_m^2, \quad m = 1, 2, 3, \dots
 \end{aligned} \tag{1.3.5}$$

Problem 2:

The additional boundary conditions are the following:

Both tangent components of velocity are prescribed on the inflow parts S_l^1 and the pressure is given on S_m^2 together with a condition on the sign of the normal component of the velocity vector. The whole formulation for problem 2 is therefore as follows:

Find a solution of equation (1.3.1) in domain Q with initial conditions (1.3.2) and the following boundary conditions

$$\begin{aligned}
 S^0 : \quad & (\mathbf{u} \cdot \mathbf{n}) = 0, \quad (\mathbf{x}, t) \in S^0. \\
 S_l^1 : \quad & (\mathbf{u} \cdot \mathbf{n}) = g_1 < 0, \quad (\mathbf{u} \cdot \boldsymbol{\tau}_i) = g_i, \quad i = 2, 3, \quad (\mathbf{x}, t) \in S_l^1, \quad l = 1, 2, \dots \\
 S_m^2 : \quad & (\mathbf{u} \cdot \mathbf{n}) > 0; \quad P = P_2, \quad (\mathbf{x}, t) \in S_m^2, \quad m = 1, 2, 3, \dots
 \end{aligned} \tag{1.3.6}$$

Problem 3:

The additional boundary conditions are the following:

Both tangent components of velocity are prescribed on the inflow parts S_l^1 and the normal component of the velocity vector is given on the outflow parts of the boundary S_m^2 . The whole formulation for problem 3 is therefore as follows:

Find a solution of equation (1.3.1) in domain Q with initial conditions (1.3.2) and the following boundary conditions

$$\begin{aligned} S^0 : \quad (\mathbf{u} \cdot \mathbf{n}) &= 0, \quad (\mathbf{x}, t) \in S^0, \\ S_l^1 : \quad (\mathbf{u} \cdot \mathbf{n}) &= g_1 < 0, \quad (\mathbf{u} \cdot \boldsymbol{\tau}_i) = g_i, \quad i = 2, 3, \quad (\mathbf{x}, t) \in S_l^1, \quad l = 1, 2, \dots \\ S_m^2 : \quad (\mathbf{u} \cdot \mathbf{n}) &= l > 0, \quad (\mathbf{x}, t) \in S_m^2, \quad m = 1, 2, 3, \dots \end{aligned} \tag{1.3.7}$$

1.4 Review of Literatures

In this section, we present a brief review of literatures associated with the well-posed initial boundary value problems and analyze the numerical schemes for the Euler equations in the cases of incompressible fluid.

1.4.1 Theoretical Investigation of Initial Boundary Value Problems for Euler Equations

The equations governing the flow of an incompressible fluid of null viscosity called also ideal fluid have been known for more than 100 years and detailed description of this mathematical model is available for example in the book of C. K. Batchelor (1970).

In each case, the set of boundary conditions supplementing the differential equations has to be studied very carefully. The treatment of boundary conditions is strictly related to the theoretical problem of the closure of the Euler equations, i.e. defining the set of boundary conditions that, together with the initial conditions, can ensure, at least locally, a stable (well-posed) solution.

The investigation of the initial boundary problems of Euler equations was developed in the work of N. M. Gunter (1927), L. Lichtenstein (1929), W. Wolinder (1933), O. A. Laduzenskaya (1975), V. N. Yudovich (1964), T. Kato (1975), H. S. Swann (1970), R. Temam (1975) and N. E. Kochin (1950). There are sufficiently complete results for the case when fluid motion occurs within the whole space or within the volume bounded by impermeable boundaries. The situation is completely different in two dimensions and in three dimensions. The incompressible Euler equations in three dimensions are far from being understood. If the dimension is equal to two, the Cauchy problem for the incompressible Euler equations is much better understood. The fundamental series of work written by R. J. Di Perna and A. Majda (1988, 1987) on this subject include a more complete discussion of the background of this issue.

It is of interest to study the problem of fluid flow through a bounded domain with the impermeable, inflow, and outflow parts of the boundary. This

situation is not only very mathematically interesting but also corresponding to various relevant physical situations. The first result for such kind of problems was obtained by N. E. Kochin (1956). Two-dimensional unsteady problems was considered by V. I. Yudovich (1964). A. V. Kazhikhov and V. V. Ragulin (1980) studied the existence and uniqueness of the boundary value problem when on the inflow parts of the boundary was prescribed by three components of velocity or normal component of velocity and two tangent components of vorticity and on the outflow parts of the boundary was prescribed by a normal component of velocity or pressure.

1.4.2 Analyzing Numerical Schemes

Due to the large variety of situations for which numerical schemes are needed, there is a wide literature on the subject a detailed analysis of which is beyond the scope of this research. Here, we will give only a short review.

A lot of research activities are devoted to analyze the numerical schemes for the Euler equations. In general, most of the techniques are consistent with non-steady flow solutions. Special emphasis is on steady flow solutions that play an important role for assessing the validity of any computational technique, especially in the multidimensional cases. Time marching approaches allow any (steady) fluid dynamics flow problem to be formulated as a pseudo-unsteady one, where the time is to be interpreted as an evolutionary coordinate such that the use of a time marching strategy is equivalent to an iterative process, whose convergence is indeed equivalent to the existence of a steady state. A. Jameson (1983), R. Peyret and T. D. Taylor (1983) and C. Hirsch (1990).

In spite of the complexity of the Euler equations, the analysis and the design of most of successful numerical approaches are in connection with the progress of the numerical treatment of simple linear and non-linear model equations, such as the (one-dimensional) advection-diffusion equation. The milestones for the modern development of numerical schemes for solving the ideal fluid flow equations are the R. Courant-E. Isaacson-M. Rees (Courant et al., 1952), and Lax-Wendroff (1960, 1964) schemes, together with the theory of Lax (Lax and Wendroff (1960, 1964) and Lax (1972)).

Further development is necessary in order to extend the theoretical results obtained by Lax and others for one-dimensional non-linear problems to multidimensional situations. A critical survey of such effort with the emphasis on the Euler and the Navier-Stokes equations has been done by Gunzburger (1996) (see R. Peyret (1996)).

Many schemes have been derived from the Lax-Wendroff scheme, the most popular being R. W. MacCormack's (1969) (and its variants), which dated back to the 1960s. Several methods have been proposed, by assuming the separability of space and time discretization. These give rise to such (rather general) classifications: explicit or implicit schemes; single- or multistep methods as far as time integration is concerned; centered or uncentered (so called upwind methods) schemes when referring to space discretization.

In the last 5-10 years, different categories of schemes preventing the generation of numerical oscillations have been proposed (and successfully employed) following the Flux Corrected Transport (FCT) concept developed by Boris and Book(1973): the Total Variation Diminishing (TVD) concept first developed by A. Harten(1983), with the recent interpretation of A. Jameson (1983) as a Local Extremum Diminishing (LED) principle A. Jameson (1983), the Monotone Upstream Discretization MUSCL concept of B. Van Leer (1977,1979),etc.

In each case, the set of boundary conditions supplementing the different equations has to be studied very carefully.

The treatment of boundary conditions is strictly related to the theoretical problem of the closure of Euler and/or Navier–Stokes equations, i.e. defining the set of boundary conditions that, together with the initial conditions, can ensure, at least locally, a stable (well-posed) solution.

Recent work on the treatment of boundary conditions by J. C. Strikwerda(1977), C. Hirsch(1990) and T. J. Poinso and S. K. Lele(1992), has focused on the aspect on time-dependent boundary conditions in order to properly account for the interaction between inner and outer phenomena.

1.5 Survey of the Thesis

Several numerical schemes have been proposed for the calculation of incompressible inviscid flows around the body or within an enclosed domain. However, the present study will concentrate almost exclusively on “flowing-through” problem in which the governing equations are the steady Euler equations. Two quite distinct numerical methods will be considered: the first one is based on the transformation of the Euler equations to new unknown functions and new independent variables. The new unknown functions are the flow angle and the modulus of the velocity vector. The new independent variables are similar to the stream function and the potential. The second method is based on the classical stream function vorticity formulation of the Euler equations.

Chapter 2 is developed to study the two-dimensional steady “flowing-through” problem 2 and two-dimensional steady “flowing-through” problem 3. The Euler equations governing two-dimensional flows are expressed in terms of two scalar unknowns which are the flow angle and the modulus of the velocity vector. The curvilinear physical domain is mapped onto a rectangular domain in new independent variables which are similar to a stream function and a potential. The new system of three equations consists of one elliptic equation and the other two equations of hyperbolic type. The difficulty of finding the solution of this system is that we have to deal with the Goursat boundary value problem in which the boundary conditions for the hyperbolic system are prescribed at the characteristics. An iterative method is constructed to obtain the numerical solution. Hyperbolic system of the equations is solved by the method of characteristic and elliptic equation is solved by the block SOR method. The convergence of algorithm is demonstrated by comparison of calculation results on a sequence of grids.

Chapter 3 discusses the “flowing-through” problem 1 in which the normal component of the velocity vector and the tangent components of the vorticity vector are given on the inflow part of the domain boundary. We utilize the non-primitive variable formulation of the Euler equations for two-dimensional flows. The nonprimitive variables are the stream function ψ and the vorticity ω . A system of two equations is solved by the iterative method. Either the block SOR method or the Stabilizing Correction method is used to solve the elliptic equation for the stream function. The upwind approximation of convective terms is applied to find the solution of the vorticity transport equation. We describe the computational techniques for determining realistic estimate of error constant and the order of convergence of a numerical algorithm. We use these techniques to estimate the convergence constant, of the algorithm developed in this thesis. The application of the algorithm is then demonstrated for an ideal incompressible fluid flow through a channel with curved walls. Strong dependence of the pressure field on the boundary condition for vorticity is found .

In Chapter 4, the thesis is briefly reviewed and the conclusions are given.



Chapter II

Numerical Methods for Steady Flowing-Through Problems: Problem 2 and Problem 3

2.1 Introduction

In this Chapter, we study numerical methods for the solution of the “flowing-through” problems in which the governing equations are the steady Euler equations of an ideal incompressible fluid. The numerical methods are developed for fluid flow through domain with an inflow and outflow parts of the domain boundary. The two kinds of boundary value problems which having relation with problem 2 and problem 3 described in section 1.3 are studied.

We rewrite the Euler equations in terms of new unknown functions and transform it to a new curvilinear coordinate system. We solve the Euler equations by an iterative process. The convergence of the numerical algorithms is established numerically by calculation in a sequence of grids. The properties of algorithm is demonstrated for a flow of an ideal incompressible fluid through the elbow channel and the channel with curvilinear boundaries in the two-dimensional case. The main idea of a transformation and an iterative algorithm is to separate the governing equations into two subsystems, one is hyperbolic and another is elliptic. The idea of such transformation was considered by I.L. Osipov et al. (1978).

2.2 Mathematical Formulation

The fundamental equations of the two-dimensional steady incompressible ideal fluid flow are the Euler equations:

$$u \frac{\partial u}{\partial x} + v \frac{\partial u}{\partial y} = - \frac{\partial P}{\partial x} . \quad (2.2.1)$$

$$u \frac{\partial v}{\partial x} + v \frac{\partial v}{\partial y} = - \frac{\partial P}{\partial y} . \quad (2.2.2)$$

$$\frac{\partial u}{\partial x} + \frac{\partial v}{\partial y} = 0 . \quad (2.2.3)$$

where $u(x, y)$ and $v(x, y)$ are components of the velocity vector in the x and y directions respectively. $P(x, y)$ is the pressure of a fluid. Without loss of generality, we set the density equal to one ($\rho = 1$).

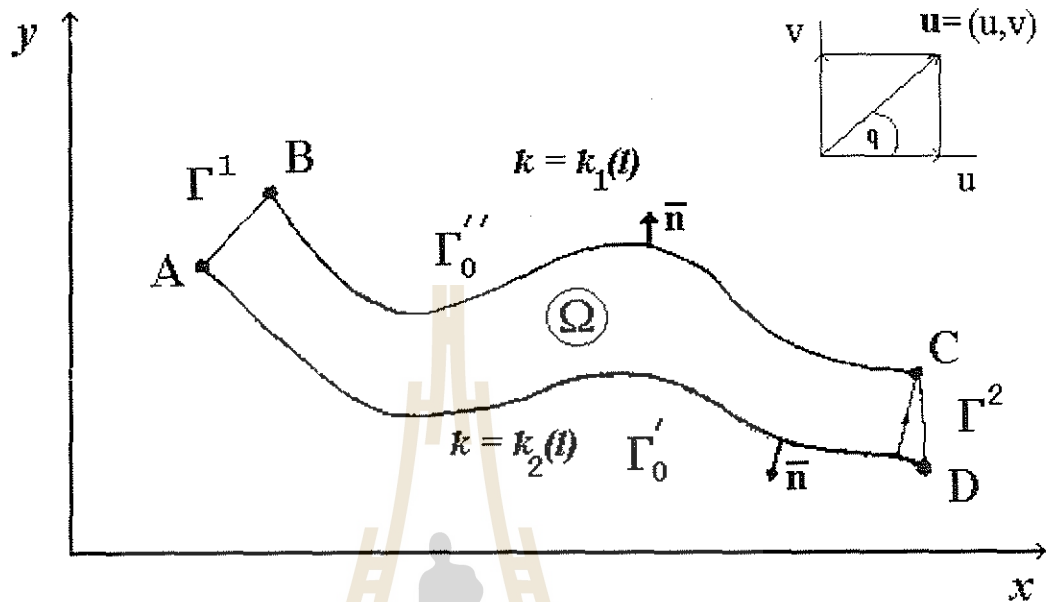


Figure 2.1: Sketch of a physical domain.

Let us assume that flow occurs in the domain Ω depicted in Figure 2.1. We assume that the solid impermeable boundaries Γ_0' and Γ_0'' are described by curves which are given by equations in the natural form

$$k = k_i(l), \quad i = 1, 2,$$

where k is the curvature and l is a natural parameter of curve.

It is convenient to rewrite the Euler equations in terms of new unknown functions $w(x, y)$ and $q(x, y)$ which are determined by the relations $u = w(x, y) \cos q(x, y)$ and $v = w(x, y) \sin q(x, y)$. Actually, $w(x, y)$ is the modulus of the velocity vector and $q(x, y)$ is the angle between the direction of the velocity vector and the Ox axis. We will call q as the flow angle. In this Chapter, we study numerical methods for two kinds of the boundary value problems.

Problem 3':

Find the solution of equations (2.2.1)–(2.2.3) with the following boundary conditions:

Impermeable boundaries AD and BC: $(x, y) \in \Gamma_0' \cup \Gamma_0''$

$$\mathbf{u} \cdot \mathbf{n} = 0. \quad (2.2.4)$$

Inflow part AB: $(x, y) \in \Gamma^1$

$$\begin{aligned} q &= q_1(x, y). \\ w &= w_1(x, y). \end{aligned} \quad (2.2.5)$$

Outflow part CD: $(x, y) \in \Gamma^2$

$$q = q_2(x, y). \quad (2.2.6)$$

Problem 2':

Find the solution of equations (2.2.1)-(2.2.3) with the following boundary conditions:

Impermeable boundaries AD and BC: $(x, y) \in \Gamma'_0 \cup \Gamma''_0$

$$\mathbf{u} \cdot \mathbf{n} = 0. \quad (2.2.7)$$

Inflow part AB: $(x, y) \in \Gamma^1$

$$\begin{aligned} q &= q_1(x, y), \\ w &= w_1(x, y). \end{aligned} \quad (2.2.8)$$

Outflow part CD: $(x, y) \in \Gamma^2$

$$\begin{aligned} P &= P_2(x, y), \\ \mathbf{u} \cdot \mathbf{n} &> 0. \end{aligned} \quad (2.2.9)$$

The problem 2' differs from the problem 3' in the boundary conditions on the outflow part CD . On CD , only pressure and condition for sign of normal component of the velocity vector are given.

2.2.1 The Euler Equations in Terms of New Unknown Function $w(x, y)$ and $q(x, y)$

In the study of the two-dimensional flow, the incompressible Euler equations can be formulated in a convenient alternative manner, by introducing two scalar variables in place of the primitive variables the velocity \bar{u} and the pressure P . The vorticity-stream function formulation has been a popular tools of computing two-dimensional incompressible flows (see, for example, P.J. Roache (1976), L. Quartapelle (1993)). Sometimes, it is convenient to use another two scalar variables which are differed from vorticity and stream function (see, for example, I.L. Osipov (1978)). In this section, we will use the modulus of the velocity and the flow angle (angle between the direction of velocity vector and the direction of Ox axis) as two new unknown functions instead the primitive variables.

We eliminate the pressure from the Euler equations by eliminating the mixed derivatives. Taking the derivatives in equations (2.2.1) and (2.2.2) with respect to y and x , respectively, we obtain

$$\left(\frac{\partial u}{\partial y}\right) \left(\frac{\partial u}{\partial x}\right) + u \frac{\partial^2 u}{\partial x \partial y} + \left(\frac{\partial v}{\partial y}\right) \left(\frac{\partial u}{\partial y}\right) + v \frac{\partial^2 u}{\partial y^2} = -\frac{\partial^2 P}{\partial x \partial y}.$$

$$\left(\frac{\partial u}{\partial x}\right)\left(\frac{\partial v}{\partial x}\right) + u\frac{\partial^2 v}{\partial x^2} + \left(\frac{\partial v}{\partial x}\right)\left(\frac{\partial v}{\partial y}\right) + v\frac{\partial^2 v}{\partial x\partial y} = -\frac{\partial^2 P}{\partial y\partial x}.$$

Then, we eliminate the terms containing the pressure by subtracting these two equations and use the condition

$$\frac{\partial^2 P}{\partial x\partial y} = \frac{\partial^2 P}{\partial y\partial x}.$$

We have

$$\begin{aligned} & \left(\frac{\partial u}{\partial y}\right)\left(\frac{\partial u}{\partial x}\right) + u\frac{\partial^2 u}{\partial x\partial y} + \left(\frac{\partial v}{\partial y}\right)\left(\frac{\partial u}{\partial y}\right) + v\frac{\partial^2 u}{\partial y^2} \\ & - \left(\frac{\partial u}{\partial x}\right)\left(\frac{\partial v}{\partial x}\right) - u\frac{\partial^2 v}{\partial x^2} - \left(\frac{\partial v}{\partial x}\right)\left(\frac{\partial v}{\partial y}\right) - v\frac{\partial^2 v}{\partial x\partial y} = 0. \end{aligned} \quad (2.2.10)$$

Substitution of $u = w(x, y) \cos q(x, y)$ and $v = w(x, y) \sin q(x, y)$ into continuity equation (2.2.3) yields

$$\frac{\partial w}{\partial x} \cos q - w \sin q \frac{\partial q}{\partial x} + \frac{\partial w}{\partial y} \sin q + w \cos q \frac{\partial q}{\partial y} = 0. \quad (2.2.11)$$

On the other hand, substitution of the expressions $u = w(x, y) \cos q(x, y)$ and $v = w(x, y) \sin q(x, y)$ into equation (2.2.10) gives us the following equation

$$\begin{aligned} & -4 \cos q w \sin q \frac{\partial w}{\partial y} \frac{\partial q}{\partial x} - 4 w \cos q \sin q \left(\frac{\partial q}{\partial y}\right)\left(\frac{\partial w}{\partial x}\right) - 4 w (\cos q)^2 \left(\frac{\partial w}{\partial x}\right)\frac{\partial q}{\partial x} \\ & + 2 w^2 \cos q \sin q \left(\frac{\partial q}{\partial x}\right)^2 - w \cos q \sin q \left(\frac{\partial^2 w}{\partial x^2}\right) - 4 w^2 (\cos q)^2 \left(\frac{\partial q}{\partial y}\right)\left(\frac{\partial q}{\partial x}\right) \\ & - 2 w^2 \cos q \sin q \frac{\partial^2 q}{\partial x\partial y} + 4 w (\cos q)^2 \left(\frac{\partial q}{\partial y}\right)\left(\frac{\partial w}{\partial y}\right) - 2 w^2 \cos q \sin q \left(\frac{\partial q}{\partial y}\right)^2 \\ & + w \cos q \sin q \frac{\partial^2 w}{\partial y^2} - w^2 \frac{\partial^2 q}{\partial y^2} - \left(\frac{\partial w}{\partial y}\right)\left(\frac{\partial w}{\partial x}\right) - w \frac{\partial^2 w}{\partial x\partial y} + 2 (\cos q) \left(\frac{\partial w}{\partial y}\right)^2 \frac{\partial w}{\partial x} \\ & + 2 w (\cos q)^2 \frac{\partial^2 w}{\partial x\partial y} + \cos q \sin q \left(\frac{\partial w}{\partial y}\right)^2 - \cos q \sin q \left(\frac{\partial w}{\partial x}\right)^2 - w^2 (\cos q)^2 \frac{\partial^2 q}{\partial x^2} \\ & + w^2 (\cos q)^2 \left(\frac{\partial^2 q}{\partial y^2}\right) + 2 w^2 \left(\frac{\partial q}{\partial y}\right)\left(\frac{\partial q}{\partial x}\right) + w \left(\frac{\partial w}{\partial x}\right)\left(\frac{\partial q}{\partial x}\right) - 3 w \left(\frac{\partial q}{\partial y}\right)\left(\frac{\partial w}{\partial y}\right) = 0. \end{aligned} \quad (2.2.12)$$

Differentiating equation (2.2.11) with respect to x and y , we obtain

$$\cos q \frac{\partial^2 w}{\partial x^2} - 2 \sin q \left(\frac{\partial w}{\partial x}\right)\left(\frac{\partial q}{\partial x}\right) - w \cos q \left(\frac{\partial q}{\partial x}\right)^2 - w \sin q \frac{\partial^2 q}{\partial x^2} + \sin q \frac{\partial^2 w}{\partial x\partial y}$$

$$+ \cos q \left(\frac{\partial w}{\partial y} \right) \left(\frac{\partial q}{\partial x} \right) + \cos q \left(\frac{\partial w}{\partial x} \right) \left(\frac{\partial q}{\partial y} \right) - w \sin q \left(\frac{\partial q}{\partial y} \right) \left(\frac{\partial q}{\partial x} \right) + w \cos q \frac{\partial^2 q}{\partial x \partial y} = 0.$$

$$\begin{aligned} & \cos q \frac{\partial^2 w}{\partial x \partial y} - \sin q \left(\frac{\partial w}{\partial x} \right) \left(\frac{\partial q}{\partial y} \right) - \sin q \left(\frac{\partial w}{\partial y} \right) \left(\frac{\partial q}{\partial x} \right) - w \cos q \left(\frac{\partial q}{\partial y} \right) \left(\frac{\partial q}{\partial x} \right) \\ & - w \sin q \frac{\partial^2 q}{\partial x \partial y} + \sin q \frac{\partial^2 w}{\partial y^2} + 2 \cos q \left(\frac{\partial w}{\partial y} \right) \left(\frac{\partial q}{\partial y} \right) - w \sin q \left(\frac{\partial q}{\partial y} \right)^2 + w \cos q \frac{\partial^2 q}{\partial y^2} = 0. \end{aligned}$$

Then, we use these two equations together to find $\frac{\partial^2 q}{\partial x \partial y}$ and $\frac{\partial^2 w}{\partial x \partial y}$. After that, substitute the value of mixed derivatives into equation (2.2.12). we get the following

$$\begin{aligned} & -w^2 \frac{\partial^2 q}{\partial y^2} - \left(\frac{\partial w}{\partial x} \right) \left(\frac{\partial w}{\partial y} \right) - 3w \left(\frac{\partial w}{\partial y} \right) \left(\frac{\partial q}{\partial y} \right) - \underline{2w \cos q \sin q \left(\frac{\partial q}{\partial y} \right) \left(\frac{\partial w}{\partial x} \right)} \\ & - 2w^2 (\cos q)^2 \left(\frac{\partial q}{\partial x} \right) \left(\frac{\partial q}{\partial y} \right) - w \left(\frac{\partial q}{\partial x} \right) \left(\frac{\partial w}{\partial x} \right) + 2w (\cos q)^2 \left(\frac{\partial q}{\partial y} \right) \left(\frac{\partial w}{\partial y} \right) \\ & - w^2 \cos q \sin q \left(\frac{\partial q}{\partial y} \right)^2 - \underline{2w (\cos q)^2 \left(\frac{\partial w}{\partial x} \right) \left(\frac{\partial q}{\partial x} \right) + w^2 \cos q \sin q \left(\frac{\partial q}{\partial x} \right)^2} \\ & - 2w \cos q \sin q \left(\frac{\partial w}{\partial y} \right) \left(\frac{\partial q}{\partial x} \right) + 2 (\cos q)^2 \left(\frac{\partial w}{\partial y} \right) \left(\frac{\partial w}{\partial x} \right) + \underline{\cos q \sin q \left(\frac{\partial w}{\partial y} \right)^2} \\ & \underline{- \cos q \sin q \left(\frac{\partial w}{\partial x} \right)^2} - w^2 \frac{\partial^2 q}{\partial x^2} + w^2 \left(\frac{\partial q}{\partial x} \right) \left(\frac{\partial q}{\partial y} \right) = 0. \end{aligned} \tag{2.2.13}$$

To eliminate the terms underlined, it is convenient to use continuity equation (2.2.11). The multiplication of equation (2.2.11) by $\frac{\partial w}{\partial x} \sin q$ gives us the value of $\left(\frac{\partial w}{\partial x} \right)^2 \cos q \sin q$. The multiplication of equation (2.2.11) by $\frac{\partial w}{\partial y} \cos q$ gives us the value of $\left(\frac{\partial w}{\partial y} \right)^2 \cos q \sin q$. The multiplication of equation (2.2.11) by $w \cos q \frac{\partial q}{\partial x}$ gives us the value of $w (\cos q)^2 \left(\frac{\partial w}{\partial x} \right) \left(\frac{\partial q}{\partial x} \right)$. The multiplication of equation (2.2.11) by $w \sin q \frac{\partial q}{\partial y}$ gives us the value of $w \cos q \sin q \left(\frac{\partial w}{\partial x} \right) \left(\frac{\partial q}{\partial y} \right)$. Then the substituting these values, $\left(\frac{\partial w}{\partial x} \right)^2 \cos q \sin q$, $\left(\frac{\partial w}{\partial y} \right)^2 \cos q \sin q$, $w (\cos q)^2 \left(\frac{\partial w}{\partial x} \right) \left(\frac{\partial q}{\partial x} \right)$ and

$w \cos q \sin q \left(\frac{\partial w}{\partial x} \right) \left(\frac{\partial q}{\partial y} \right)$, into equation (2.2.13) instead of the terms underlined. after simplification, we obtain

$$\frac{\partial}{\partial x} \left(w^2 \frac{\partial q}{\partial x} \right) + \frac{\partial}{\partial y} \left(w^2 \frac{\partial q}{\partial y} \right) = 0. \quad (2.2.14)$$

All above algebraic manipulation are done by MAPLE program. The detailed MAPLE program can be found in Appendix A.

2.2.2 Transformation from Cartesian Coordinates (x, y) to Generalized Curvilinear Coordinates (φ, ψ)

The computation of flow fields in and around complex shapes such as ducts, engine, complete aircraft or automobiles, etc., involves computational boundaries that do not coincide with coordinate lines in a physical domain. For finite difference methods, the imposition of boundary conditions for such problems motivate the introduction of a mapping or transformation from a physical (x, y) domain to a generalized curvilinear coordinate space. The generalize coordinate domain is constructed so that a computational boundary in a physical domain coincides with a coordinate line in a generalized coordinate space.

The use of generalized coordinates implies that a distorted region in a physical domain is mapped into a rectangular region in the generalized coordinate space as shown in Figure 2.2.

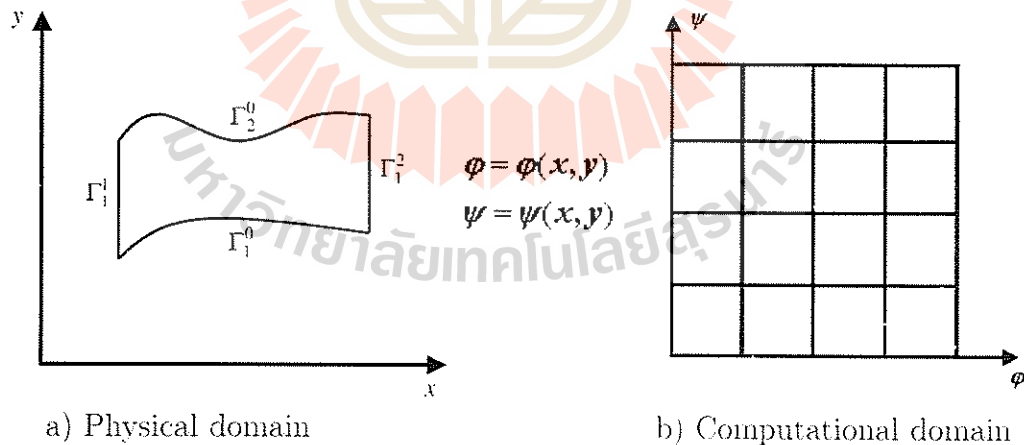


Figure 2.2: Physical and computational domain.

Next, we introduce new independent variables φ and ψ . We will choose ψ which is similar to a stream function and φ as an independent function which is similar to the potential. It is assumed that there is a unique, single-valued relationship between the generalized coordinates and the physical coordinates

which can be written as

$$\varphi = \varphi(x, y), \quad \psi = \psi(x, y) \quad (2.2.15)$$

and by implication

$$x = x(\varphi, \psi), \quad y = y(\varphi, \psi).$$

The specific relationship is given by the equations for total differentials of φ and ψ , respectively

$$d\varphi = \varphi_x dx + \varphi_y dy = \frac{\cos q}{\phi} dx + \frac{\sin q}{\phi} dy, \quad (2.2.16)$$

$$d\psi = \psi_x dx + \psi_y dy = -c\psi \sin q dx + c\psi \cos q dy. \quad (2.2.17)$$

In equations (2.2.16) and (2.2.17), c is a constant, and $\phi(x, y)$ is a new unknown function. These values are chosen such that the new variables (φ, ψ) are functionally independent, i.e. the Jacobian is not equal to zero

$$J(x, y) = \frac{\partial(\varphi, \psi)}{\partial(x, y)} = \frac{c\psi}{\phi} \neq 0.$$

Equation (2.2.16) has to determine unique function $\varphi(x, y)$. It means that the mixed derivatives are equal, i.e.

$$\frac{\partial^2 \varphi(x, y)}{\partial x \partial y} = \frac{\partial^2 \varphi(x, y)}{\partial y \partial x}. \quad (2.2.18)$$

Substitution of $\frac{\partial \varphi}{\partial y}$ and $\frac{\partial \varphi}{\partial x}$ from (2.2.16) into equation (2.2.18) gives the equation

$$\frac{\partial}{\partial x} \left(\frac{\sin q(x, y)}{\phi(x, y)} \right) = \frac{\partial}{\partial y} \left(\frac{\cos q(x, y)}{\phi(x, y)} \right). \quad (2.2.19)$$

Equation (2.2.19) may be used as an additional equation for the new unknown function $\phi(x, y)$. From equations (2.2.16) and (2.2.17), we have the value of partial derivatives

$$\begin{aligned} \frac{\partial \varphi}{\partial y} &= \frac{\sin q}{\phi(x, y)}; & \frac{\partial \varphi}{\partial x} &= \frac{\cos q}{\phi(x, y)}; \\ \frac{\partial \psi}{\partial x} &= -c\psi \sin q; & \frac{\partial \psi}{\partial y} &= c\psi \cos q. \end{aligned} \quad (2.2.20)$$

To transform the system of equations (2.2.11), (2.2.14) and (2.2.19) to new independent variables, we need to know the values of $\frac{\partial x}{\partial \varphi}$, $\frac{\partial x}{\partial \psi}$, $\frac{\partial y}{\partial \varphi}$ and $\frac{\partial y}{\partial \psi}$. It is easy to show that

$$\begin{bmatrix} \frac{\partial \varphi}{\partial x} & \frac{\partial \varphi}{\partial y} \\ \frac{\partial \psi}{\partial x} & \frac{\partial \psi}{\partial y} \end{bmatrix} \begin{bmatrix} \frac{\partial x}{\partial \varphi} & \frac{\partial x}{\partial \psi} \\ \frac{\partial y}{\partial \varphi} & \frac{\partial y}{\partial \psi} \end{bmatrix} = \begin{bmatrix} 1 & 0 \\ 0 & 1 \end{bmatrix}.$$

Really, we have

$$\begin{aligned} dx &= \frac{\partial x}{\partial \varphi} d\varphi + \frac{\partial x}{\partial \psi} d\psi, \\ dy &= \frac{\partial y}{\partial \varphi} d\varphi + \frac{\partial y}{\partial \psi} d\psi \end{aligned}$$

or in a matrix form

$$\begin{bmatrix} dx \\ dy \end{bmatrix} = \begin{bmatrix} \frac{\partial x}{\partial \varphi} & \frac{\partial x}{\partial \psi} \\ \frac{\partial y}{\partial \varphi} & \frac{\partial y}{\partial \psi} \end{bmatrix} \begin{bmatrix} d\varphi \\ d\psi \end{bmatrix}.$$

Solving this matrix equation, for the right-hand column matrix, we have

$$\begin{bmatrix} d\varphi \\ d\psi \end{bmatrix} = \begin{bmatrix} \frac{\partial x}{\partial \varphi} & \frac{\partial x}{\partial \psi} \\ \frac{\partial y}{\partial \varphi} & \frac{\partial y}{\partial \psi} \end{bmatrix}^{-1} \begin{bmatrix} dx \\ dy \end{bmatrix}$$

This matrix form can be compared with the matrix form

$$\begin{bmatrix} d\varphi \\ d\psi \end{bmatrix} = \begin{bmatrix} \frac{\partial \varphi}{\partial x} & \frac{\partial \varphi}{\partial y} \\ \frac{\partial \psi}{\partial x} & \frac{\partial \psi}{\partial y} \end{bmatrix} \begin{bmatrix} dx \\ dy \end{bmatrix}$$

Therefore

$$\begin{bmatrix} \frac{\partial \varphi}{\partial x} & \frac{\partial \varphi}{\partial y} \\ \frac{\partial \psi}{\partial x} & \frac{\partial \psi}{\partial y} \end{bmatrix} = \begin{bmatrix} \frac{\partial x}{\partial \varphi} & \frac{\partial x}{\partial \psi} \\ \frac{\partial y}{\partial \varphi} & \frac{\partial y}{\partial \psi} \end{bmatrix}^{-1}$$

Following the standard rules for finding the inverse matrix, this equation is written as follows

$$\begin{bmatrix} \frac{\partial x}{\partial \varphi} & \frac{\partial x}{\partial \psi} \\ \frac{\partial y}{\partial \varphi} & \frac{\partial y}{\partial \psi} \end{bmatrix} = \frac{\begin{bmatrix} \frac{\partial \psi}{\partial y} & -\frac{\partial \varphi}{\partial y} \\ -\frac{\partial \psi}{\partial x} & \frac{\partial \varphi}{\partial x} \end{bmatrix}}{\begin{vmatrix} \frac{\partial \varphi}{\partial x} & \frac{\partial \varphi}{\partial y} \\ \frac{\partial \psi}{\partial x} & \frac{\partial \psi}{\partial y} \end{vmatrix}}$$

or

$$\begin{bmatrix} \frac{\partial x}{\partial \varphi} & \frac{\partial x}{\partial \psi} \\ \frac{\partial y}{\partial \varphi} & \frac{\partial y}{\partial \psi} \end{bmatrix} = \frac{1}{J} \begin{bmatrix} \frac{\partial \psi}{\partial y} & -\frac{\partial \varphi}{\partial y} \\ -\frac{\partial \psi}{\partial x} & \frac{\partial \varphi}{\partial x} \end{bmatrix} \quad (2.2.21)$$

where the Jacobian J is defined as

$$J = \frac{\partial(\varphi, \psi)}{\partial(x, y)} = \begin{vmatrix} \frac{\partial\varphi}{\partial x} & \frac{\partial\varphi}{\partial y} \\ \frac{\partial\psi}{\partial x} & \frac{\partial\psi}{\partial y} \end{vmatrix} = \frac{cw \cos^2 q}{\phi} + \frac{cw \sin^2 q}{\phi} = \frac{cw}{\phi} \neq 0.$$

Since the Jacobian $J \neq 0$, then ϕ and w are not equal to zero. Finally, we can rewrite (2.2.21) in the form

$$\begin{aligned} \frac{\partial x}{\partial\varphi} &= \frac{1}{J}\psi_y = \phi \cos q, & \frac{\partial x}{\partial\psi} &= -\frac{1}{J}\varphi_y = -\frac{\sin q}{cw}, \\ \frac{\partial y}{\partial\varphi} &= -\frac{1}{J}\psi_x = \phi \sin q, & \frac{\partial y}{\partial\psi} &= \frac{1}{J}\varphi_x = \frac{\cos q}{cw}. \end{aligned} \quad (2.2.22)$$

2.2.3 The Equations in New Generalized Curvilinear Coordinates (φ, ψ)

The first step: We transform the continuity equation (2.2.3). Substitution of $u = w \cos q$ and $v = w \sin q$ into this equation yields

$$\frac{\partial w \cos q}{\partial x} + \frac{\partial w \sin q}{\partial y} = 0$$

or

$$\cos q \frac{\partial w}{\partial x} - w \sin q \frac{\partial q}{\partial x} + \sin q \frac{\partial w}{\partial y} + w \cos q \frac{\partial q}{\partial y} = 0. \quad (2.2.23)$$

By using the chain rule, we have the formulas to change partial derivatives

$$\begin{aligned} \frac{\partial(\cdot)}{\partial x} &= \frac{\partial(\cdot)}{\partial\varphi} \frac{\partial\varphi}{\partial x} + \frac{\partial(\cdot)}{\partial\psi} \frac{\partial\psi}{\partial x} = \frac{\cos q}{\phi} \frac{\partial(\cdot)}{\partial\varphi} - cw \sin q \frac{\partial(\cdot)}{\partial\psi}, \\ \frac{\partial(\cdot)}{\partial y} &= \frac{\partial(\cdot)}{\partial\varphi} \frac{\partial\varphi}{\partial y} + \frac{\partial(\cdot)}{\partial\psi} \frac{\partial\psi}{\partial y} = \frac{\sin q}{\phi} \frac{\partial(\cdot)}{\partial\varphi} + cw \cos q \frac{\partial(\cdot)}{\partial\psi}. \end{aligned} \quad (2.2.24)$$

Substituting equations (2.2.24) into equation (2.2.23) and making simplifications, we get

$$\begin{aligned} &\frac{(\cos q)^2}{\phi} \frac{\partial w}{\partial\varphi} - cw \cos q \sin q \frac{\partial w}{\partial\psi} - w \frac{\cos q}{\phi} \sin q \frac{\partial q}{\partial\varphi} + cw^2 (\sin q)^2 \frac{\partial q}{\partial\psi} \\ &+ \frac{(\sin q)^2}{\phi} \frac{\partial w}{\partial\varphi} + cw \cos q \sin q \frac{\partial w}{\partial\psi} + w \frac{\sin q}{\phi} \cos q \frac{\partial q}{\partial\varphi} + cw^2 (\cos q)^2 \frac{\partial q}{\partial\psi} = 0 \end{aligned}$$

or

$$\frac{1}{\phi} [(\cos q)^2 + (\sin q)^2] \frac{\partial w}{\partial\varphi} + cw^2 [(\cos q)^2 + (\sin q)^2] \frac{\partial q}{\partial\psi} = 0$$

or

$$\frac{1}{\phi} \frac{\partial w}{\partial \varphi} + cw^2 \frac{\partial q}{\partial \psi} = 0.$$

which can be arranged into

$$\frac{\partial}{\partial \varphi} \left(\frac{1}{w} \right) = c\phi \frac{\partial q}{\partial \psi}. \quad (2.2.25)$$

The second step: We have to use the condition

$$\frac{\partial^2 \varphi}{\partial x \partial y} = \frac{\partial^2 \varphi}{\partial y \partial x}. \quad (2.2.26)$$

Substitution of $\frac{\partial \varphi}{\partial y}$ and $\frac{\partial \varphi}{\partial x}$ from equation (2.2.20) yields

$$\frac{\partial}{\partial y} \left(\frac{\cos q}{\phi} \right) = \frac{\partial}{\partial x} \left(\frac{\sin q}{\phi} \right) \quad (2.2.27)$$

or

$$-\phi \sin q \frac{\partial q}{\partial y} - \cos q \frac{\partial \phi}{\partial y} = \phi \cos q \frac{\partial q}{\partial x} - \sin q \frac{\partial \phi}{\partial x}.$$

Substituting equations (2.2.24) into equation (2.2.7) and making simplifications, we get the following equation in the term of new variables

$$\frac{\partial \phi}{\partial w} = \frac{1}{cw} \frac{\partial q}{\partial \varphi}. \quad (2.2.28)$$

The third step: Substituting partial derivatives from equations (2.2.24) into equation

$$\frac{\partial}{\partial x} \left(w^2 \frac{\partial q}{\partial x} \right) + \frac{\partial}{\partial y} \left(w^2 \frac{\partial q}{\partial y} \right) = 0.$$

we obtain

$$\frac{\partial}{\partial x} \left(w^2 \frac{\cos q}{\phi} \frac{\partial q}{\partial \varphi} - cw^3 \sin q \frac{\partial q}{\partial \psi} \right) + \frac{\partial}{\partial y} \left(w^2 \frac{\sin q}{\phi} \frac{\partial q}{\partial \varphi} + cw^3 \cos q \frac{\partial q}{\partial \psi} \right) = 0.$$

By simplifying, we get then the equation in the terms of new variables as follows

$$\frac{\partial}{\partial \varphi} \left(\frac{w^2}{\phi} \frac{\partial q}{\partial \varphi} \right) + c^2 w \phi \frac{\partial}{\partial \psi} \left(w^3 \frac{\partial q}{\partial \psi} \right) = 0. \quad (2.2.29)$$

In order to transform equations (2.2.1), (2.2.3) and (2.2.26) to equations (2.2.25), (2.2.28) and (2.2.29), a program by MAPLE is developed the detailed description of this program can be found in Appendix A.

We have to find the image of fluid domain in the new variables (φ, ψ) . It is clear that impermeable boundaries Γ'_0 , Γ''_0 (AD and BC) are streamlines

and $\psi|_{AD}$ and $\psi|_{BC}$ are constants. The function $\psi(x, y)$ is determined up to an arbitrary constant, and without loss of generality, we can choose

$$\psi|_{BC} = 0.$$

Then we have

$$\psi|_{AD} = \psi(A) = \text{const.}$$

We can take the curvilinear integral of $d\psi$ along the boundary AB (see Figure 2.1) to estimate the value of $\psi(A)$ through the given values of w and q on the boundary AB

$$\int_A^B d\psi = \int_A^B [v_x dx + v_y dy] = \int_{AB} [-cw_1 \sin q_1 dx + cw_1 \cos q_1 dy]$$

where functions $w_1(x, y)$, $q_1(x, y)$ are given by boundary conditions (2.2.5). We can rewrite the previous equation in the form

$$\psi(B) - \psi(A) = c \left[\int_A^B [-w_1 \sin q_1 dx + w_1 \cos q_1 dy] \right].$$

If we choose the value of the constant c as

$$c = \frac{1}{\left[\int_A^B [-w_1 \sin q_1 dx + w_1 \cos q_1 dy] \right]}$$

and take into account that $\psi(B) = 0$, we obtain

$$\psi(A) = -1.$$

It means that the image of boundary AD is an interval of straight line

$$\psi|_{AD} = -1.$$

Now we have to find the image of AB and CD . Let us assume that equation of boundary AB is given in the explicit form

$$y = y_{AB}(x) \tag{2.2.30}$$

or in the differential form

$$dy = y'_{AB}(x) dx$$

then

$$dy - y'_{AB}(x) dx = 0. \tag{2.2.31}$$

Substitution of equalities

$$\begin{aligned} dy &= y_\varphi d\varphi + y_v dv, \\ dx &= x_\varphi d\varphi + x_v dv \end{aligned}$$

into equation (2.2.31) yields

$$(y_\psi - y'_{AB}(x)x_\psi) d\varphi + (y_\varphi - y'_{AB}(x)x_\varphi) d\psi = 0. \quad (2.2.32)$$

We assume that the image of AB is given by the equation

$$\varphi = \varphi_{A'B'}(\psi). \quad (2.2.33)$$

In (φ, ψ) -plane, equation (2.2.32) is ODE for unknown function $\varphi_{A'B'}(\psi)$

$$\frac{d\varphi_{A'B'}(\psi)}{d\psi} = -\frac{y_\psi - y'_{AB}(x)x_\psi}{y_\varphi - y'_{AB}(x)x_\varphi}. \quad (2.2.34)$$

Substitution of y_ψ , x_ψ , y_φ , x_φ from equations (2.2.22) gives

$$\varphi'_{A'B'}(\psi) = -\frac{\cos q_1 + y'_{AB}(x) \sin q_1}{c \phi w_1 (\sin q_1 - y'_{AB}(x) \cos q_1)}. \quad (2.2.35)$$

The function $\varphi_{A'B'}(\psi)$ is a new unknown and may be calculated from equation (2.2.35). In some particular practical cases, equation (2.2.35) has an analytical solution. These cases can be illustrated by the following examples:

Example 1: Let us assume that

$$y_{AB}(x) = \text{const and } q_1 = \pi/2.$$

It is clear that in this case

$$\frac{d\varphi_{A'B'}(\psi)}{d\psi} = 0,$$

therefore

$$\varphi_{A'B'}(\psi) = \text{const.}$$

Because $\varphi_{A'B'}(0) = 0$, we get

$$\varphi_{A'B'}(\psi) = 0.$$

Example 2: Let us assume that

$$y_{AB}(x) = lx + m$$

and fluid entering into domain by right angle, i.e.

$$\cos q_1 + y'_{AB}(x) \sin q_1 = 0.$$

In this case, again we have

$$\frac{d\varphi_{A'B'}(\psi)}{d\psi} = 0.$$

therefore

$$\varphi_{A'B'}(\psi) = 0.$$

Let us consider boundary CD . In the case of problem 3', we know the values of flow angle at the boundary CD

$$q(x, y) = q_2(x, y), \quad (x, y) \in \Gamma^2.$$

Let us assume that equation of boundary CD is given in the explicit form

$$x = x_{CD}(y),$$

or in the differential form

$$dx = x'_{CD}(y)dy,$$

then

$$dx - x'_{CD}(y)dy = 0. \quad (2.2.36)$$

Substitution of equalities

$$dy = y_\varphi d\varphi + y_\psi d\psi,$$

$$dx = x_\varphi d\varphi + x_\psi d\psi,$$

into equation (2.2.36) yields

$$(x_\varphi - x'_{CD}(y)y_\varphi)d\varphi + (x_\psi - x'_{CD}(y)y_\psi)d\psi = 0. \quad (2.2.37)$$

We assume that image of CD is given by the equation

$$\varphi = \varphi_{C'D'}(\psi).$$

In (φ, ψ) - plane equation (2.2.37) is ODE for unknown function $\varphi_{C'D'}(\psi)$

$$\frac{d\varphi_{C'D'}(\psi)}{d\psi} = \frac{x_\psi - x'_{CD}(y)y_\psi}{x_\varphi - x'_{CD}(y)y_\varphi},$$

or

$$\varphi'_{C'D'}(\psi) = \frac{\sin q_2 + x'_{CD}(y) \cos q_2}{c w \phi (\cos q_2 - x'_{CD}(y) \sin q_2)}. \quad (2.2.38)$$

In some particular cases the function $\varphi_{C'D'}(\psi)$ has simple form. These cases can be illustrated by the following example:

Example 3: Let us assume that

$$x_{CD}(y) = \text{const.} \quad \text{and} \quad q_2 = 0.$$

It is clear that in this case

$$\frac{d\varphi_{C'D'}(\psi)}{d\psi} = 0.$$

therefore

$$\varphi_{C'D'}(\psi) = \text{const.}$$

and due to $\varphi_{C'D'}(0) = 1$, we get

$$\varphi_{C'D'}(\psi) = 1.$$

In the case of problem 2', we know the pressure at the boundary CD . $P(x, y) = P_2(x, y)$, $(x, y) \in \Gamma_2$. Here, the situation is slightly more complicated. Let us assume that equation of boundary $C'D'$ is given by the formula

$$\varphi = \varphi_{C'D'}(\psi)$$

and the equation of boundary CD is given by the formula

$$y = y_{CD}(x).$$

By analogy with two previous cases, we have

$$\varphi'_{C'D'}(\psi) = -\frac{\cos q + y'_{CD}(x) \sin q}{c \phi w_2 (\sin q - y'_{CD}(x) \cos q)}. \quad (2.2.39)$$

Main difference between formulas (2.2.38) and (2.2.39) is that values of q in (2.2.39) are still unknown on boundary CD . To get equation for q on CD , we have to use two equations (2.2.1) and (2.2.2). Let us consider a particular case when equation of boundary CD is $x = x_0 - \text{const}$ and $P = P_2(y) = \text{const}$, $y \in CD$. In this case we have

$$u \frac{\partial v}{\partial x} + v \frac{\partial v}{\partial y} = -\frac{\partial P}{\partial y} = 0. \quad (2.2.40)$$

Substitution of $u = w \cos q(x, y)$ and $v = w \sin q(x, y)$ into equation (2.2.40) and simplification with help of continuity equation (2.2.3) yield

$$\frac{\partial q}{\partial \varphi} = c \phi w \tan q \frac{\partial q}{\partial \psi}, \quad (\varphi, \psi) \in C'D'. \quad (2.2.41)$$

We must use equation (2.2.41) as the boundary condition for q on boundary $C'D'$.

Now we have to derive boundary condition for function $\phi = \phi(x, y)$. The new unknown function ϕ subject to the condition that the Jacobian $J(x, y) = \frac{cw}{\phi}$ is not equal to zero or infinity. This function also has to satisfy equation (2.2.27). The boundary conditions for $\phi(x, y)$ are arbitrary. We can put $\phi(x, y) = \phi_0 - \text{const}$ on the streamline BC. Then we can integrate equation (2.2.16)

$$d\varphi = \frac{1}{\phi} (\cos q dx + \sin q dy)$$

along the streamline BC

$$\int_{B'C'} d\varphi = \int_{B'}^{C'} \frac{1}{\phi} (\cos q dx + \sin q dy)$$

or

$$\varphi(C') - \varphi(B') = \frac{1}{\phi_0} L_{BC}$$

where L_{BC} is the length of boundary BC . If we choose $\phi_0 = L_{BC}$ and take into account that $\varphi(B') = 0$, we obtain

$$\varphi(C') = 1.$$

In order to summarize, we write the formulation of problem 3' and problem 2' in a compact form in terms of new unknown functions and new independent variables (φ, ψ).

Problem 3':

We have to find the simultaneous solutions of the following set of partial differential equations

$$\frac{\partial}{\partial \varphi} \left(\frac{1}{w} \right) = c\phi \frac{\partial q}{\partial \psi} \quad (2.2.42)$$

$$\frac{\partial \phi}{\partial \psi} = -\frac{1}{cw} \frac{\partial q}{\partial \varphi} \quad (2.2.43)$$

$$\frac{\partial}{\partial \varphi} \left(\frac{w^2}{\phi} \frac{\partial q}{\partial \varphi} \right) + c^2 w \phi \frac{\partial}{\partial \psi} \left(w^3 \frac{\partial q}{\partial \psi} \right) = 0 \quad (2.2.44)$$

in the domain $A'B'C'D'$ depicted in Figure 2.3.

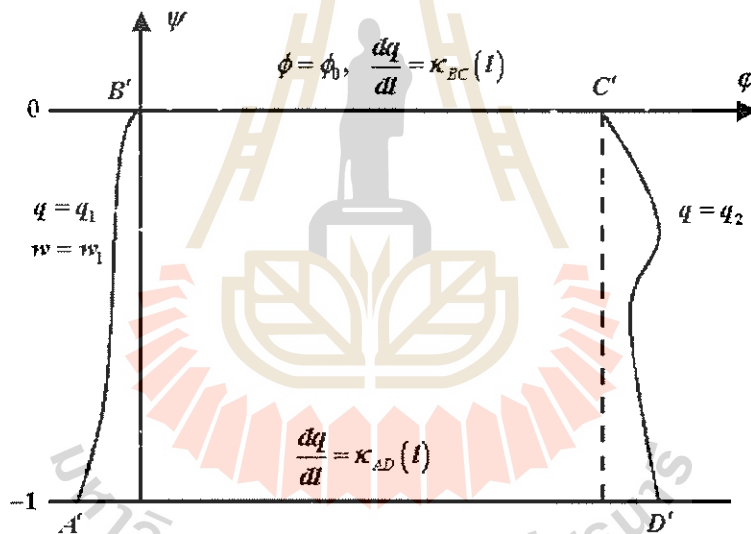


Figure 2.3: Domain $A'B'C'D'$ for problem 3'.

Equations (2.2.42)–(2.2.44) have to satisfy the following boundary conditions.

$$\begin{aligned}
A'B' : \quad \frac{d\varphi_{A'B'}}{d\psi} &= -\frac{\cos q_1 + y'_{AB}(x) \sin q_1}{c \phi w_1 (\sin q_1 - y'_{AB}(x) \cos q_1)}; \psi \in [0, -1] \\
\varphi_{A'B'}(0) &= 0, \\
q &= q_1(\varphi, \psi), \quad \varphi = \varphi_{A'B'}(\psi) \\
w &= w_1(\varphi, \psi), \quad \varphi = \varphi_{A'B'}(\psi)
\end{aligned} \tag{2.2.45}$$

$$\begin{aligned}
B'C' : \quad \phi(\varphi, 0) &= \phi_0, \quad \phi_0 \neq 0, \\
\frac{dq}{dl} &= k_{BC}(l),
\end{aligned} \tag{2.2.46}$$

$$\begin{aligned}
C'D' : \quad q &= q_2(\varphi, \psi), \quad \varphi = \varphi_{C'D'}(\psi) \\
\frac{d\varphi_{C'D'}}{d\psi} &= -\frac{\cos q_2 + y'_{CD}(x) \sin q_2}{c \phi w_2 (\sin q_2 - y'_{CD}(x) \cos q_2)}; \psi \in [0, -1] \\
\varphi_{C'D'}(0) &= 1
\end{aligned} \tag{2.2.47}$$

$$A'D' : \quad \frac{dq}{dl} = k_{AD}(l), \tag{2.2.48}$$

where $k_{AD}(l)$ and $k_{BC}(l)$, as functions of the length l along the curve are curvature of boundaries AD and BC .

Problem 2':

We have to find the simultaneous solutions of equations (2.2.42)–(2.2.44) in the domain $A'B'C'D'$ depicted in Figure 2.4 with boundary conditions

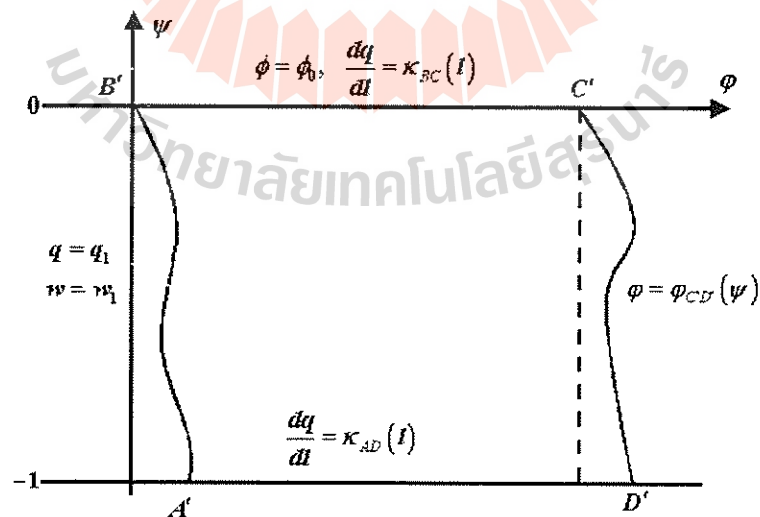


Figure 2.4: Domain $A'B'C'D'$ for problem 2'

$$\begin{aligned}
A'B' : \quad \frac{d\varphi_{A'B'}}{d\psi} &= -\frac{\cos q_1 + y'_{AB}(x) \sin q_1}{c \phi w_1 (\sin q_1 - y'_{AB}(x) \cos q_1)}; \psi \in [0, -1] \\
\varphi_{A'B'}(0) &= 0 \\
q &= q_1(\varphi, \psi), \quad \varphi = \varphi_{A'B'}(\psi) \\
w &= w_1(\varphi, \psi), \quad \varphi = \varphi_{A'B'}(\psi)
\end{aligned} \tag{2.2.49}$$

$$\begin{aligned}
B'C' : \quad \phi(\varphi, 0) &= \phi_0, \quad \phi_0 \neq 0, \\
\frac{dq}{dl} &= k_{BC}(l),
\end{aligned} \tag{2.2.50}$$

$$\begin{aligned}
C'D' : \quad \frac{d\varphi_{C'D'}}{d\psi} &= -\frac{\cos q + y'_{CD}(x) \sin q}{c \phi w_2 (\sin q - y'_{CD}(x) \cos q)}; \psi \in [0, -1] \\
\varphi_{C'D'}(0) &= 1,
\end{aligned} \tag{2.2.51}$$

$$\frac{\partial q}{\partial \varphi} = c \phi w \tan q \frac{\partial q}{\partial \psi}, \quad (\varphi, \psi) \in C'D'$$

$$A'D' : \quad \frac{dq}{dl} = k_{AD}(l),$$

where $k_{AD}(l)$ and $k_{BC}(l)$, as functions of the length l along the curve are curvature of boundaries AD and BC .

2.3 Discretization of the Equations and the Solution Procedure

To explain the numerical procedure, we restrict ourself to the case of problem 3'. In this case, domain $A'B'C'D'$ is the uniform rectangular domain. In the case of the problem 2', we can use new variables

$$\begin{aligned}
\tilde{\psi} &= \psi, \\
\tilde{\varphi} &= \frac{\varphi - \varphi_{A'B'}(\psi)}{\varphi_{C'D'}(\psi) - \varphi_{A'B'}(\psi)}
\end{aligned}$$

to transform domain $A'B'C'D'$ into a rectangular domain. For a moment, we assume that the function q is given. Then equations (2.2.42) or (2.2.43) are the hyperbolic system of equations with respect to w and ϕ . We have the Goursat problem for the system of equations (2.2.42) and (2.2.43) with w is given on $A'B'$ and ϕ is known on $B'C'$. If we assume that w and ϕ are known then equation (2.2.44) is elliptic with respect to q . By virtue of this note, we will create an iterative process.

In domain $A'B'C'D'$, we construct a uniform rectangular finite difference grid $\Omega_h = \{(\psi_i, \varphi_j), \psi_i = -1 + (i-1)h_\psi, \varphi_j = (j-1)h_\varphi, i = 1, \dots, N_1;$

$j = 1, \dots, N_2\}$. All unknown functions are approximated at the nodes of grid. To calculate the solution of equations (2.2.42)-(2.2.44). we design the following iterative process:

- Suppose we know $q^{(n-1)}$, $w^{(n-1)}$ and $\phi^{(n-1)}$ from the previous iteration or from the initial guess.
- The solution of equations (2.2.42) and (2.2.43) with $q = q^{(n-1)}$ is evaluated by the method of characteristics.
- When the values $w^{(n)}$ and $\phi^{(n)}$ are found. we solve equation (2.2.44) by either the block SOR or the Stabilizing Correction method.

For finding the solution of equations (2.2.42) and (2.2.43) by the method of characteristic. the partial derivatives of $q(x, y)$ are taken from the $(n-1)$ -st iteration. On each line $\psi = \text{const}$ and $\varphi = \text{const}$ the Modified Euler Predictor-Corrector method (see J. D. Hoffman (1992)) is used. The derivatives $\frac{\partial q^{(n-1)}}{\partial \psi}$ and $\frac{\partial q^{(n-1)}}{\partial \varphi}$ are approximated by the central finite differences. At the boundary, these derivatives are approximated by one-sided finite differences of second order. The Predictor-Corrector method consists of the following two steps:

The first step (Predictor) is

$$\begin{aligned} \frac{\left(\frac{1}{w^*}\right)_{i,j} - \left(\frac{1}{w^{(n-1)}}\right)_{i,j-1}}{h_\varphi} &= -c \phi_{i,j-1}^{(n-1)} \left(\delta_h q_\psi^{(n-1)}\right)_{i,j-1}, \\ & i = 1, \dots, N_1, \quad j = 2, \dots, N_2 \\ \frac{\phi_{i+1,j}^{(n-1)} - \phi_{i,j}^*}{h_\psi} &= -\frac{1}{c w_{i+1,j}^{(n-1)}} \left(\delta_h q_\varphi^{(n-1)}\right)_{i+1,j}, \\ & i = N_1 - 1, \dots, 1, \quad j = 1, \dots, N_2. \end{aligned}$$

The second step (Corrector) is

$$\begin{aligned} \frac{\left(\frac{1}{w^*}\right)_{i,j} - \left(\frac{1}{w^{(n-1)}}\right)_{i,j-1}}{h_\varphi} &= \frac{1}{2} \left[c \phi_{i,j}^* \left(\delta_h q_\psi^{(n-1)}\right)_{i,j} + c \phi_{i,j-1}^{(n-1)} \left(\delta_h q_\psi^{(n-1)}\right)_{i,j-1} \right], \\ & i = 1, \dots, N_1, \quad j = 2, \dots, N_2 \\ \frac{\phi_{i+1,j}^{(n-1)} - \phi_{i,j}^{(n)}}{h_\psi} &= \frac{1}{2} \left[-\frac{1}{c w_{i,j}^*} \left(\delta_h q_\varphi^{(n-1)}\right)_{i,j} - \frac{1}{c w_{i+1,j}^{(n-1)}} \left(\delta_h q_\varphi^{(n-1)}\right)_{i+1,j} \right], \\ & i = N_1 - 1, \dots, 1, \quad j = 1, \dots, N_2. \end{aligned}$$

Here the superscript (*) denotes the results of the predictor, and δ_h denotes the second order approximation of corresponding derivatives q_φ or q_ψ . Before to perform calculations in this stage, we have to calculate ϕ on line $A'B'$ and w on the boundary $B'C''$ by using the equation

$$\frac{\partial \phi}{\partial \psi} = -\frac{1}{c w_1} \frac{\partial q}{\partial \varphi}.$$

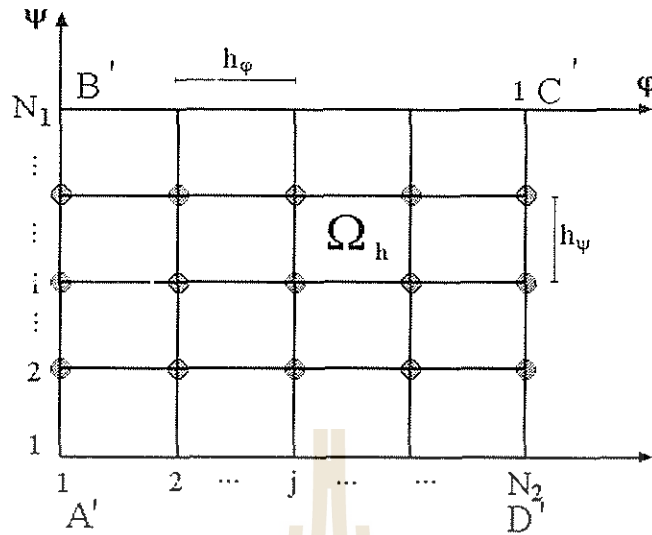


Figure 2.5: Sketch of finite difference grid.

$$o_{ij} = o(\varphi_j, \psi_i), \quad \psi_i = -1 + h_\psi(i-1), \quad \varphi_j = (j-1)h_\varphi.$$

Let us assume, for simplicity, that $w_1 = \text{const.}$ Integrating this equation with respect to ψ from ψ_i to 0, we get

$$\int_{\psi_i}^0 \frac{\partial \phi}{\partial \psi} = -\frac{1}{c w_1} \int_{\psi_i}^0 \frac{\partial q}{\partial \varphi} d\varphi,$$

$$o(0,0) - o(0, \psi_i) = -\frac{1}{c w_1} \int_{\psi_i}^0 (q_\varphi) d\psi,$$

or in the difference form

$$o_{i,1} = o_{N_1,1} + \frac{1}{c w_1} \int_{\psi_i}^0 q(\varphi) d\psi, \quad i = N_1 - 1, N_1 - 2, \dots, 1.$$

For $i = N_1 - 1$, we can approximate the last equation as follows

$$o_{N_1-1,1} \approx o_{N_1,1} + \frac{1}{2 c w_1} \left[(q_\varphi)_{N_1,1} + (q_\varphi)_{N_1-1,1} \right] h_1,$$

where $h_1 = \psi_{i+1} - \psi_i$. Here, to estimate $\int_{\psi_{N_1-1}}^0 (q_\varphi) d\psi$, we use the trapezoidal rule. For the case $i < N_1 - 1$ we use the Simpson formula of fourth order to

approximate the integral $\int_{v_i}^{v_{i+2}} (q_\varphi) dv$

$$\begin{aligned} \mathcal{O}_{i,1} &= \mathcal{O}_{N_1,1} + \frac{1}{c w_1} \left[\int_{v_{i-2}}^0 (q_\varphi) dv + \int_{v_i}^{v_{i+2}} (q_\varphi) dv \right] \\ &= \mathcal{O}_{i+2,1} + \frac{1}{c w_1} \int_{v_i}^{v_{i+2}} (q_\varphi) dv \\ &\approx \mathcal{O}_{i+2,1} + \frac{1}{6 c w_1} \left[(q_\varphi)_i + 4 (q_\varphi)_{i+1} + (q_\varphi)_{i+2} \right] h_1. \\ & \quad i = N_1 - 2, \dots, 1. \end{aligned}$$

Equation (2.2.42) is used to find $w(x, y)$ along boundary BC' . Integrating equation (2.2.42) with respect to φ from 0 to φ_j , we get

$$\begin{aligned} \int_0^{\varphi_j} \frac{\partial}{\partial \varphi} \left(\frac{1}{w} \right) d\varphi &= c \mathcal{O}_0 \int_0^{\varphi_j} \frac{\partial q}{\partial \psi} d\varphi. \\ \frac{1}{w_{N_1,j}} - \frac{1}{w_{N_1,1}} &= c \mathcal{O}_0 \int_0^{\varphi_j} \frac{\partial q}{\partial \psi} d\varphi. \quad j = 2, \dots, N_2 \end{aligned} \quad (2.3.1)$$

For the case $j=2$, we approximate the right hand side of equation (2.3.1) by the trapezoidal rule

$$\frac{1}{w_{N_1,2}} \approx \frac{1}{w_{N_1,1}} + \frac{1}{2} c \mathcal{O}_0 \left[(q_\psi)_{N_1,1} + (q_\psi)_{N_1,2} \right] h_2.$$

For the case $j > 2$, we use the Simpson formula of fourth order to approximate integral $\int_{\varphi_j}^{\varphi_{j+2}} (q_\psi) d\varphi$

$$\begin{aligned} \frac{1}{w_{N_1,j}} &= \frac{1}{w_{N_1,1}} + c \mathcal{O}_0 \left[\int_0^{\varphi_{j-2}} (q_\psi) d\varphi + \int_{\varphi_{j-2}}^{\varphi_j} (q_\psi) d\varphi \right] \\ &= \frac{1}{w_{N_1,j-2}} + c \mathcal{O}_0 \left[\int_{\varphi_{j-2}}^{\varphi_j} (q_\psi) d\varphi \right] \\ &\approx \frac{1}{w_{N_1,j-2}} + \frac{c \mathcal{O}_0}{6} \left[(q_\psi)_j + 4 (q_\psi)_{j-1} + (q_\psi)_{j-2} \right] h_2. \\ & \quad j = 3, \dots, N_2. \end{aligned}$$

where $h_2 = \varphi_{j-1} - \varphi_j$. The partial derivatives $\frac{\partial q}{\partial v}$ and $\frac{\partial q}{\partial \varphi}$ are approximated by the second order central difference and by one side second order difference near edge points A', C', B'

$$\left(\frac{\partial q}{\partial v} \right)_{i,j_0} = \begin{cases} \frac{1}{2} \frac{q_{i+1,j_0} - q_{i-1,j_0}}{h_1}, & i \neq 1 \text{ and } i \neq N_1. \\ \frac{1}{2} \frac{3q_{N_1,j_0} - 4q_{N_1-1,j_0} + q_{N_1-2,j_0}}{h_1}, & i = N_1. \\ \frac{1}{2} \frac{-3q_{1,j_0} + 4q_{2,j_0} - q_{3,j_0}}{h_1}, & i = 1. \end{cases}$$

$$\left(\frac{\partial q}{\partial \varphi}\right)_{i_0,j} = \begin{cases} \frac{1}{2} \frac{q_{i_0,j+1} - q_{i_0,j-1}}{h_2}; & j \neq 1 \text{ and } j \neq N_2, \\ \frac{1}{2} \frac{3q_{i_0,N_2} - 4q_{i_0,N_2-1} + q_{i_0,N_2-2}}{h_2}; & j = N_2, \\ \frac{1}{2} \frac{-3q_{i_0,1} + 4q_{i_0,2} - q_{i_0,3}}{h_2}; & j = 1. \end{cases}$$

When the values $w^{(n)}$ and $\phi^{(n)}$ are found for all grid points, we can solve equation (2.2.44). Before to perform calculations in this stage, we have to find $q^{(n)}$ on the boundaries $B'C'$ and $A'D'$. Due to the boundary condition imposed on $\phi(x, y)$ at the boundary BC , we have

$$d\varphi = \frac{1}{\phi_0}(\cos q dx + \sin q dy) = \frac{1}{\phi_0} dl \quad (2.3.2)$$

where ϕ_0 is nonzero constant and l is the natural parameter of curve AD . Let us integrate (2.3.2) from 0 to $\varphi_j = (j-1)h_\varphi$

$$\int_0^{\varphi_j} d\varphi = \frac{1}{\phi_0} \int_0^{\varphi_j} dl$$

or

$$\varphi_j = \frac{1}{\phi_0} l_j$$

where l_j is length of curve BC from the point which corresponds to $\varphi_1 = 0$ to the point which corresponds to $\varphi = \varphi_j$. To find q_j we can use natural equation of curve BC (see E. V. Shikin(1995))

$$\frac{dq}{dl} = k_{BC}(l).$$

where $k_{BC}(l)$ is equation of curve BC in natural form. Integrating this equations with respect to l from 0 to l_j we get

$$q_{1,j} - q_{N_1,0} = \int_0^{l_j} k_{BC}(l) dl.$$

It is important to remark that the boundary condition for q at boundary BC has to be estimated only once before starting the iterative process. On the boundary AD we do not know the exact values of $\phi(\varphi, \psi)$. The boundary condition for q on the boundary AD has to be involved into the outer iterative process. In this case we have

$$\phi(\psi, \varphi) d\varphi = dl,$$

or after integration

$$l_j = \int_0^{\varphi_j} \phi^{(n)}(\psi, \varphi) d\varphi, \quad \psi = -1.$$

Utilizing the natural equation of boundary AD , we obtain

$$\frac{d\tilde{q}^{(n)}}{dl} = k_{AD}(l).$$

or after integration

$$\tilde{q}_{1,j}^{(n)} - \tilde{q}_{1,0}^{(n)} = \int_0^{l_j} k_{AD}(l) dl$$

where $\tilde{q}^{(n)}$, $\phi^{(n)}$ denote the values on n -th iteration.

For the sake of simplicity, either the block SOR or the Stabilizing Corrections method (see N. N. Yanenko(1971)) is used to find the approximate solution $\tilde{q}^{(n)}$ of equation (2.2.44). We utilize the second order central differences to approximate the partial derivatives. The system of tridiagonal linear algebraic equations is solved by the "sweep method" (see for example N. N. Yanenko(1971)). Relaxation is needed to achieve the convergence

$$q_{ij}^{(n)} = q_{ij}^{(n-1)} + \omega(\tilde{q}_{ij}^{(n)} - q_{ij}^{(n-1)}). \quad (2.3.3)$$

The relaxation factor ω is chosen by trial and error method. The iterative process is terminated when the convergence criterion is achieved

$$\begin{aligned} \max_{i,j \in \Omega_h} \left| \frac{q_{ij}^{(n)} - q_{ij}^{(n-1)}}{q_{ij}^{(n)}} \right| &< \epsilon_q, \\ \max_{i,j \in \Omega_h} \left| \frac{\phi_{ij}^{(n)} - \phi_{ij}^{(n-1)}}{\phi_{ij}^{(n)}} \right| &< \epsilon_\phi, \\ \max_{i,j \in \Omega_h} \left| \frac{w_{ij}^{(n)} - w_{ij}^{(n-1)}}{w_{ij}^{(n)}} \right| &< \epsilon_w, \end{aligned} \quad (2.3.4)$$

where ϵ_q , ϵ_ϕ and ϵ_w are the convergence tolerances. A flowchart of the iterative process is presented in Figure 2.6. It is needed to point that there are also efficient numerical methods to solve equation (2.2.44) such as some direct method, preconditioning techniques, etc.. However, these methods require more storage than the relaxation methods or fractional step methods and also they are more complicated to develop a computing programme. For convenience, we write the formulas of the block SOR method as well as formulas of the Stabilizing Correction method.

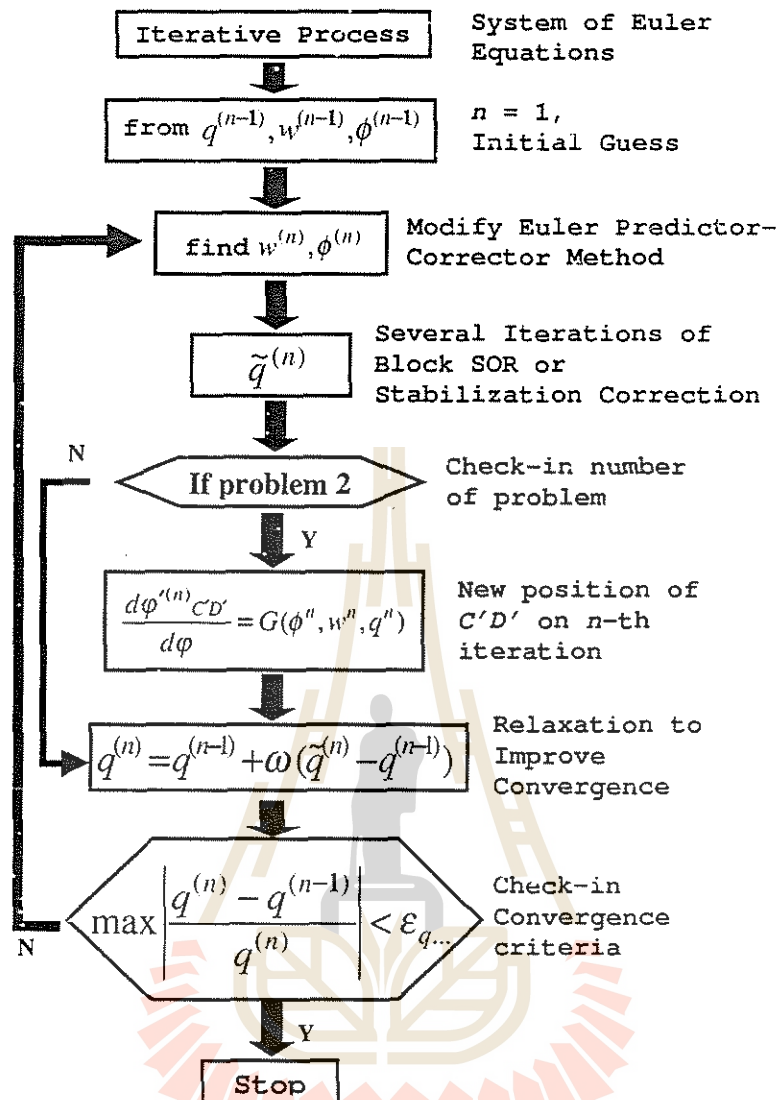


Figure 2.6: Flowchart of the iterative process.

2.3.1 The Method of Block SOR

The solution of equation (2.2.29) is sought in the domain shown in Figure 2.7. A three-point finite difference discretization of equation (2.2.29) is

$$\begin{aligned}
 & \frac{(w^2/\phi)_{i,j+1/2} \left(q_{i,j+1}^{(n-1)} - \tilde{q}_{i,j} \right) - (w^2/\phi)_{i,j-1/2} \left(\tilde{q}_{i,j} - q_{i,j-1}^{(n-1)} \right)}{h_\phi^2} + \\
 & \frac{c^2 w_{ij} \phi_{ij} \left(w_{i+1/2,j}^3 (\tilde{q}_{i+1,j} - \tilde{q}_{i,j}) - w_{i-1/2,j}^3 (\tilde{q}_{i,j} - \tilde{q}_{i-1,j}) \right)}{h_w^2} = 0. \quad (2.3.5)
 \end{aligned}$$

$$i = 2, \dots, N_1 - 1, \quad j = 2, \dots, N_2 - 1,$$

where $w_{i,j\pm 1/2} = \frac{1}{2}(w_{i,j\pm 1} + w_{i,j})$, $w_{i\pm 1/2,j} = \frac{1}{2}(w_{i\pm 1,j} + w_{i,j})$ and $\tilde{q}_{i,j}$ is the intermediate values of the unknown vector q .

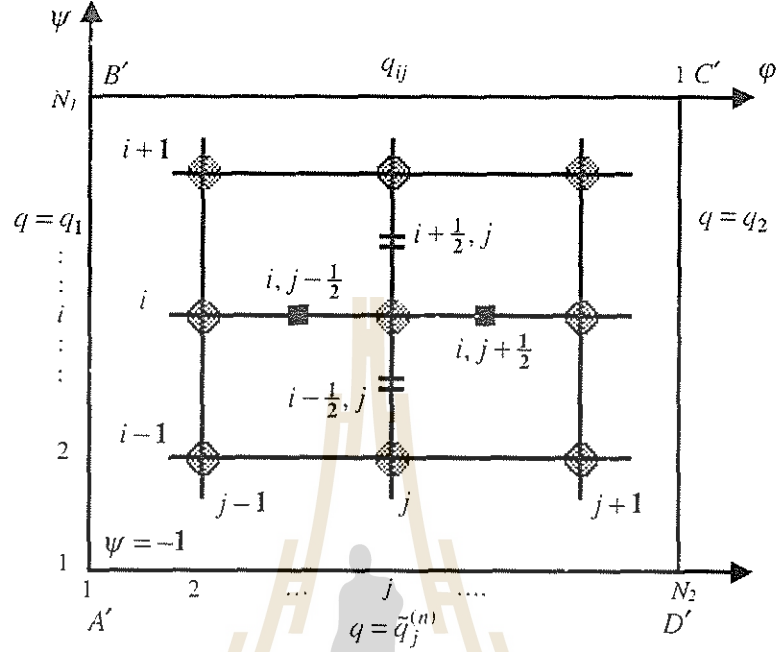


Figure 2.7: Computational stencil for finite difference equation (2.3.5).

We can rewrite equation (2.3.5) in the form of a linear system of algebraic equations with a tridiagonal matrix

$$-A_i \tilde{q}_{i-1,j} + C_i \tilde{q}_{i,j} - B_i \tilde{q}_{i+1,j} = f_{i,j}. \quad (2.3.6)$$

$$i = 2, \dots, N_1 - 1, \quad j = 2, \dots, N_2 - 1.$$

where

$$A_i = c^2 w_{ij} \phi_{ij} w_{i-1/2,j}^3 \frac{1}{h_\psi^2}.$$

$$B_i = c^2 w_{ij} \phi_{ij} w_{i+1/2,j}^3 \frac{1}{h_\psi^2}.$$

$$C_i = \left[\left(\frac{w^2}{\phi} \right)_{i,j+1/2} + \left(\frac{w^2}{\phi} \right)_{i,j-1/2} \right] \frac{1}{h_\psi^2} + A_i + B_i.$$

$$f_{i,j} = \frac{1}{h_\psi^2} \left[\left(\frac{w^2}{\phi} \right)_{i,j+1/2} q_{i,j+1}^{(n-1)} + \left(\frac{w^2}{\phi} \right)_{i,j-1/2} q_{i,j-1}^{(n-1)} \right].$$

The sweep method for the solution of (2.3.6) is given by the following formulas

$$\begin{aligned}\tilde{q}_{i,j} &= \alpha_{i+1}\tilde{q}_{i+1,j} + \beta_{i+1}, \\ i &= 1, \dots, N_1 - 1, \\ j &= 2, \dots, N_2 - 1, \\ \alpha_{i+1} &= \frac{\beta_i}{C_i - A_i\alpha_i}: \quad i = 2, \dots, N_1 - 1, \\ \beta_{i+1} &= \frac{f_{ij} + A_i\beta_i}{C_i - A_i\alpha_i}: \quad i = 2, \dots, N_1 - 1, \\ \tilde{q}_{N_1,j} &= \tilde{q}_{BC}(j), \\ \tilde{q}_{1,j} &= \tilde{q}_{AD}(j).\end{aligned}$$

In the SOR scheme, the solution of (2.3.6) is combined with the solution in the previous iteration $q_{ij}^{(n-1)}$

$$q_{ij}^{(n)} = \lambda\tilde{q}_{ij} + (1 - \lambda)q_{ij}^{(n-1)}, \quad i = 1, \dots, N_1, \quad j = 1, \dots, N_2, \quad (2.3.7)$$

where λ is the relaxation factor. The SOR method in the range $0 < \lambda < 2$ produces a sequence of convergent solutions.

2.3.2 The Method of Stabilizing Corrections

The method of Stabilizing Corrections which was introduced by J. Douglas and H. H. Rachford (1956) and formulated into a general form by J. Douglas and J. E. Gunn (1964) is a very effective method for the construction of scheme with fractional step. It consists of two fractional steps

$$\begin{aligned}\frac{q_{ij}^* - q_{ij}^{(n-1)}}{\tau} &= \frac{(w^2/\phi)_{i,j+1/2}(q_{i,j+1}^* - q_{ij}^*) - (w^2/\phi)_{i,j-1/2}(q_{ij}^* - q_{i,j-1}^*)}{h_\phi^2} \\ &+ c^2 w_{ij} \phi_{ij} \frac{w_{i+1/2,j}^3 (q_{i+1,j}^{(n-1)} - q_{ij}^{(n-1)}) - w_{i-1/2,j}^3 (q_{ij}^{(n-1)} - q_{i-1,j}^{(n-1)})}{h_\psi^2}, \quad (2.3.8) \\ i &= 2, \dots, N_1 - 1, \quad j = 2, \dots, N_2 - 1,\end{aligned}$$

$$\begin{aligned}\frac{q_{ij}^{(n)} - q_{ij}^*}{\tau} &= c^2 w_{ij} \phi_{ij} \left[\frac{w_{i+1/2,j}^3 (q_{i+1,j}^{(n)} - q_{ij}^{(n)}) - w_{i-1/2,j}^3 (q_{ij}^{(n)} - q_{i-1,j}^{(n)})}{h_\psi^2} \right. \\ &\left. + \frac{w_{i+1/2,j}^3 (q_{i+1,j}^{(n-1)} - q_{ij}^{(n-1)}) - w_{i-1/2,j}^3 (q_{ij}^{(n-1)} - q_{i-1,j}^{(n-1)})}{h_\phi^2} \right]. \quad (2.3.9) \\ i &= 2, \dots, N_1 - 1, \quad j = 2, \dots, N_2 - 1.\end{aligned}$$

To find solution of equations (2.3.8) and (2.3.9), we have to solve a linear system of an algebraic equations with the tridiagonal matrix.

2.3.3 Interpretation and Presentation of Results of Numerical Calculations

In this section, we discuss how to display the results of numerical calculations. We will use various generally accepted graphical techniques for the

presentation of data. Presentations of results in the physical domain are more desirable. When the iterative process is completed, we have to transform back to the variables x, y to find distribution of all unknown functions in the physical domain.

Let us consider the line $v = v_i - \text{const}$ (streamline). Along this line we have

$$\frac{dx(\varphi, v_i)}{d\varphi} = o(\varphi, v_i) \cos q(\varphi, v_i).$$

Integrating this equation with respect to φ from $\varphi = 0$ to $\varphi = \varphi_j$, we obtain

$$\int_0^{\varphi_j} dx(\varphi, v_i) = \int_0^{\varphi_j} o(\varphi, v_i) \cos q(\varphi, v_i) d\varphi,$$

or

$$\begin{aligned} x_{i,j} - x_{1,j} &= x(\varphi_j, v_i) - x(0, v_i) \\ &= \int_0^{\varphi_j} o(\varphi, v_i) \cos q(\varphi, v_i) d\varphi, \end{aligned}$$

where $x_{1,j} = x(0, v_i)$ is x coordinate of the point $(0, v_i)$ in the physical domain. To find $x_{1,j}$, consider the image of Γ_1 boundary in a particular case where

$$AB : y = y_0 - \text{const}, x_0 \leq x \leq x_1. \quad (2.3.10)$$

In this case, we have (see equation (2.2.17))

$$\frac{dv}{dx} = -c w(0, v) \sin q(0, v).$$

Integrating this equation with respect from 0 to v_i , we get

$$- \int_0^{v_i} \frac{dv}{c w(0, v) \sin q(0, v)} = x_{1,i} - x_{1,1},$$

or

$$x_{1,i} = x_{1,1} - \int_0^{v_i} \frac{dv}{c w(0, v) \sin q(0, v)},$$

where the functions $w(0, v)$ and $\sin q(0, v)$ are given by the boundary conditions $q = q_1(x, y)$ and $w = w_1(x, y)$. By analogy with the previous case, we can find y - coordinates $y_{i,j}$ of the streamline $v = v_{i,j}$: $j = 1, \dots, N_2$.

$$\frac{dy(\varphi, v_i)}{d\varphi} = o(\varphi, v_i) \sin q(\varphi, v_i).$$

Integration yields

$$y(\varphi_j, v_i) = y(0, v_i) + \int_0^{\varphi_j} o(\varphi, v_i) \sin q(\varphi, v_i) d\varphi.$$

In particular case of boundary condition (2.3.10), it is easy to see that

$$y(0, v_i) = y_0.$$

Once the unknown functions q , w , ϕ are determined, it is possible to find distribution of the pressure in the physical and computational domain. To find the pressure, we use equations (2.2.1) and (2.2.2)

$$\begin{aligned} u \frac{\partial u}{\partial x} + v \frac{\partial u}{\partial y} &= -\frac{\partial P}{\partial x} \\ u \frac{\partial v}{\partial x} + v \frac{\partial v}{\partial y} &= -\frac{\partial P}{\partial y} \end{aligned} \quad (2.3.11)$$

Utilizing the chain rule, we receive formulas to change the partial derivatives

$$\begin{aligned} \frac{\partial P}{\partial x} &= -c w \frac{\partial P}{\partial w} \sin q + \frac{\partial P \cos q}{\partial \varphi \phi} \\ \frac{\partial P}{\partial y} &= c w \frac{\partial P}{\partial w} \cos q + \frac{\partial P \sin q}{\partial \varphi \phi} \end{aligned}$$

Multiplying the first equation by $\sin q$ and the second equation by $\cos q$, then by subtraction, we get

$$-c w \frac{\partial P}{\partial w} = \frac{\partial P}{\partial x} \sin q - \frac{\partial P}{\partial y} \cos q. \quad (2.3.12)$$

Multiplying the first equation by $\cos q$ and the second equation by $\sin q$, then by addition, we get

$$\frac{1}{\phi} \frac{\partial P}{\partial \varphi} = \frac{\partial P}{\partial x} \cos q + \frac{\partial P}{\partial y} \sin q. \quad (2.3.13)$$

Substituting $\frac{\partial P}{\partial x}$ and $\frac{\partial P}{\partial y}$ into equations (2.3.12) and (2.3.13), we get

$$-c w \frac{\partial P}{\partial w} = -\left(u \frac{\partial u}{\partial x} + v \frac{\partial u}{\partial y}\right) \sin q + \left(u \frac{\partial v}{\partial x} + v \frac{\partial v}{\partial y}\right) \cos q \quad (2.3.14)$$

$$\frac{1}{\phi} \frac{\partial P}{\partial \varphi} = -\left(u \frac{\partial u}{\partial x} + v \frac{\partial u}{\partial y}\right) \cos q - \left(u \frac{\partial v}{\partial x} + v \frac{\partial v}{\partial y}\right) \sin q. \quad (2.3.15)$$

Substituting $u = w \cos q$ and $v = w \sin q$ into equations (2.3.14) and (2.3.15) and simplifying, we obtain

$$\begin{aligned} \frac{\partial P}{\partial w} &= -\frac{w}{\phi} \frac{\partial q}{\partial \varphi} \\ \frac{\partial P}{\partial \varphi} &= -w \frac{\partial w}{\partial \varphi} \quad (\text{or } w^3 c \phi \frac{\partial q}{\partial w}). \end{aligned} \quad (2.3.16)$$

In order to transform equations (2.2.1) and (2.2.2) to equations (2.3.16), a program by MAPLE is developed. The detailed description of this program can be found in Appendix A.

Assume that the value of the pressure is given at some point of domain Ω . The pressure determine up to an arbitrary constant. We can use equations (2.3.16) to find the values of the pressure in the physical domain.

Let $P(A) = P_0$ be a given value of the pressure at the point A of boundary AB (see Figure 2.1). To find the pressure distribution along AB , we have

$$\begin{aligned}\frac{\partial P}{\partial w} &= -\frac{w}{c\phi} \frac{\partial q}{\partial \varphi}, \\ \frac{\partial P(w, 0)}{\partial w} &= -\frac{w}{c\phi(w, 0)} \left(\frac{\partial q}{\partial \varphi} \right)_{\varphi=0}, \\ \int_A^{w_i} \frac{\partial P(w, 0)}{\partial w} dw &= -\frac{1}{c} \int_A^{w_i} \frac{w}{\phi(w, 0)} \left(\frac{\partial q}{\partial \varphi} \right)_{\varphi=0} dw, \\ P(w_i, 0) - P(A) &= -\frac{1}{c} \int_{-1}^{w_i} \frac{w}{\phi(w, 0)} \left(\frac{\partial q}{\partial \varphi} \right)_{\varphi=0} dw: \quad P(A) = P_0, \\ P_{i,1} &= P_0 - \frac{1}{c} \left[\int_{-1}^{w_{i-1}} \frac{w}{\phi(w, -1)} \left(\frac{\partial q}{\partial \varphi} \right)_{\varphi=-1} dw \right. \\ &\quad \left. - \int_{w_{i-1}}^{w_i} \frac{w}{\phi(w, 0)} \left(\frac{\partial q}{\partial \varphi} \right)_{\varphi=0} dw \right] \\ &= P_{i-1,1} - \frac{1}{c} \int_{w_{i-1}}^{w_i} \frac{w}{\phi(w, 0)} \left(\frac{\partial q}{\partial \varphi} \right)_{\varphi=0} dw.\end{aligned}$$

where $\left(\frac{\partial q}{\partial \varphi} \right)_{\varphi=0} = \frac{-3q_{i,1} + 4q_{i,2} - q_{i,3}}{2h_2}$.

We use equation

$$\frac{\partial P}{\partial \varphi} = -w \frac{\partial w}{\partial \varphi} \quad (\text{or} \quad \frac{\partial P}{\partial \varphi} = w^3 c \phi \frac{\partial q}{\partial w}).$$

to find the pressure distribution everywhere in the computational domain. Integrating this equation, we have

$$\begin{aligned}\int_0^{\varphi_j} \frac{\partial P}{\partial \varphi} d\varphi &= -\int_0^{\varphi_j} w \frac{\partial w}{\partial \varphi} d\varphi, \\ P(w_i, \varphi_j) - P(w_i, 0) &= -\int_0^{\varphi_j} w \frac{\partial w}{\partial \varphi} d\varphi, \\ P_{i,j} &= P_{i,1} - \int_0^{\varphi_{j-1}} w \frac{\partial w}{\partial \varphi} d\varphi - \int_{\varphi_{j-1}}^{\varphi_j} w \frac{\partial w}{\partial \varphi} \Big|_{v=w_i} d\varphi \\ &= P_{i,j-1} - \int_{\varphi_{j-1}}^{\varphi_j} w \frac{\partial w}{\partial \varphi} \Big|_{v=w_i} d\varphi.\end{aligned}$$

$$i = 1, \dots, N_1.$$

$$j = 2, \dots, N_2.$$

where

$$\left(\frac{\partial w}{\partial \varphi}\right)_{i,j} = \begin{cases} \frac{w_{i,j+1} - w_{i,j-1}}{2h_2} & : j \neq N_2. \\ \frac{3w_{i,N_2} - 4w_{i,N_2-1} + w_{i,N_2-2}}{2h_2} & : j = N_2. \end{cases}$$

$$\left(\frac{\partial w}{\partial \varphi}\right)_{i,j-1} = \begin{cases} \frac{w_{i,j} - w_{i,j-2}}{2h_2} & : j \neq N_2, \\ \frac{-3w_{i,1} + 4w_{i,2} - w_{i,3}}{2h_2} & : j = 2. \end{cases}$$

2.4 Results and Discussions

In this section, the numerical method developed in section 2.3 will be implemented to study an internal flow of an ideal incompressible fluid in an α degree elbow channel and two-dimensional channel with curve walls.

2.4.1 90 Degree Elbow with Contraction

The channel geometry is shown in Figure 2.8. Parts of solid impermeable boundary FL and KE are circular arcs with centers at the points O and F , respectively. In Figure 2.8, we also show the flow domain in new variables in the case of problem 2' and problem 3'. In the case of problem 2', the image of CD boundary is not vertical. We will present this boundary $C'D'$ by the equation

$$\varphi = 1 + \varphi_{C'D'}(\psi).$$

Taking into account the natural parameterization of circle we can write out the natural equations of boundaries AD and BC . In the case of boundary BC we can write

$$x(l) = \begin{cases} -R_1, & 0 \leq l \leq y_0, \\ -R_1 + R_1 \cos\left(\frac{l-y_0}{R_1}\right), & y_0 < l < y_0 + \frac{\pi}{2}R_1, \\ l - \left(y_0 + \frac{\pi}{2}R_1\right), & y_0 + \frac{\pi}{2}R_1 \leq l \leq L_{BC}. \end{cases} \quad (2.4.1)$$

$$y(l) = \begin{cases} y_0 - l, & 0 \leq l \leq y_0, \\ -R_1 \sin\left(\frac{l-y_0}{R_1}\right), & y_0 < l < y_0 + \frac{\pi}{2}R_1, \\ -R_1, & y_0 + \frac{\pi}{2}R_1 \leq l \leq L_{BC}. \end{cases} \quad (2.4.2)$$

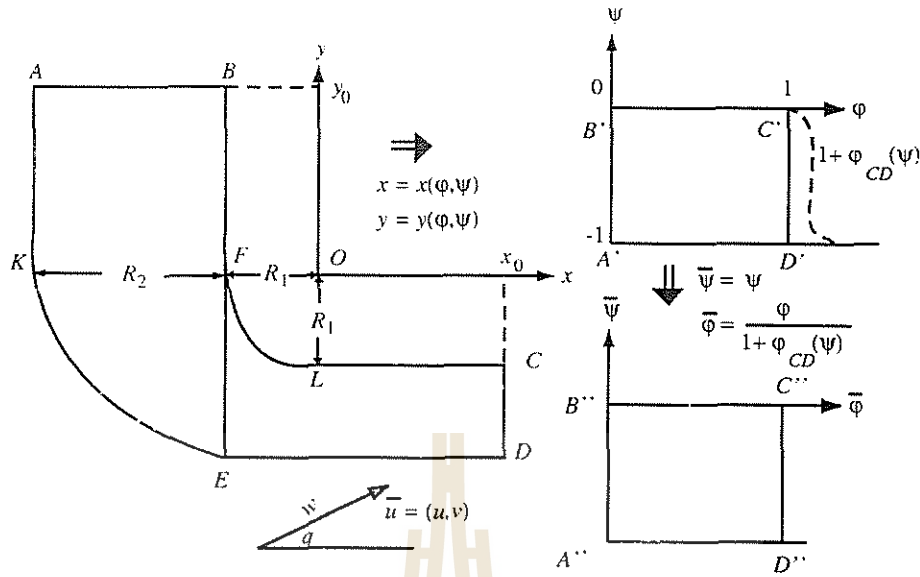


Figure 2.8: Sketch of an elbow-shaped domain and coordinates.

where l is a natural parameter of curve BC . L_{BC} is the length of curve BC . The similar description is also valid for the boundary AD

$$x(l) = \begin{cases} -(R_1 + R_2), & 0 \leq l \leq y_0. \\ -(R_1 + R_2) + R_2 \cos\left(\frac{l-y_0}{R_2}\right), & y_0 < l < y_0 + \frac{\pi}{2}R_1. \\ l - (y_0 + \frac{\pi}{2}R_1), & y_0 + \frac{\pi}{2}R_1 \leq l \leq L_{AD}. \end{cases} \quad (2.4.3)$$

$$y(l) = \begin{cases} y_0 - l, & 0 \leq l \leq y_0. \\ -R_2 \sin\left(\frac{l-y_0}{R_2}\right), & y_0 < l < y_0 + \frac{\pi}{2}R_1. \\ -R_2, & y_0 + \frac{\pi}{2}R_1 \leq l \leq L_{AD}. \end{cases} \quad (2.4.4)$$

2.4.2 Convergence of Numerical Algorithm

To prove that the solution of the numerical method converges to the solution of the partial differential equations is generally very difficult. For the equations governing fluid flow, convergence is usually impossible to demonstrate theoretically. The convergence can be demonstrated numerically by obtaining solutions on a sequence of refined grids. Convergence implies that the solution error should decrease as the grid spacing is reduced. It is clear, that in the case of 90 degree elbow with contraction, we do not know an exact solution of the Euler equations. Our algorithm developed by such way that some *priori* known quantities have to be estimated during the iterative process. For example, in the case of problem 3', we know the exact location of point D , and the exact value of length of channel's boundary AD but while the numerical process is carried out, we have to compute the quantities of these data. The corresponding rela-

tive errors between exact values of these quantities and their numerical approach are shown in Table 2.1 for the following set of parameters $R_1 = 1.0$, $R_2 = 2.0$, $x_0 = 2.0$, $y_0 = 2.0$, $w = w_1(x) = 2.0$, $q_1 = q(x, y_0) = -\pi/2$, and $q_2 = q(x_d, y) = 0$. In the first and the second columns, we present the number of grid points in the computational domain. The third and the fifth columns of Table 2.1 present the (x, y) - coordinates of point D found by numerical algorithm. The seventh column presents the length of curve AD which is found by the numerical algorithm. In the fourth, sixth and eighth columns, we demonstrate relative difference between exact and approximate values

$$\text{error} = \frac{(\cdot)\text{exact} - (\cdot)\text{approximate}}{(\cdot)\text{exact}} \times 100\%$$

It is clear to see from results in Table 2.1 that the relative errors decrease as the grid size tends to zero. The last column demonstrates the optimal value of the relaxation parameter. The optimal values of relaxation factor are chosen by method of trail and error.

Using results of Table 2.1, we can find rate of convergence of our numerical algorithm

$$m = \frac{1 - \ln(\text{err1})}{\ln(2) \ln(\text{err2})}$$

where err1 and err2 are relative error between the exact and approximate values which were obtained on grids $N1 \times N1$ and $N2 \times N2$. Rate of convergence is shown in Table 2.2.

Table 2.1: Convergence to exact solution. The results of numerical simulations for different grids for 90 degree elbow.

N_1	N_2	x_D	relative error in x_D	y_D	relative error in y_D	L_{AD}^h	relative error in L_{AD}	ω optimal
11	11	2.045695	-2.28475	-2.031267	-1.56335	8.1925	-0.6252	0.8
21	21	2.025775	-1.28875	-2.007746	-0.38730	8.1659	-0.2985	0.8
41	41	2.017319	-0.86595	-2.001790	-0.08950	8.1566	-0.1842	0.93
81	81	2.009273	-0.46365	-2.000499	-0.02495	8.1509	-0.1142	0.93
11	21	2.033372	-1.66860	-2.008183	-0.40915	8.1729	-0.3844	0.8
11	41	2.026327	-1.31635	-2.001492	-0.07460	8.1654	-0.2923	1.2
21	41	2.020008	-1.00040	-2.001718	-0.08590	8.1593	-0.2174	1.2
21	11	2.035630	-1.78150	-2.031677	-1.58385	8.1824	-0.5011	0.8
41	11	2.030568	-1.52840	-2.031859	-1.59295	8.1774	-0.4391	0.6
11	81	2.018081	-0.90405	-2.000682	-0.03410	8.1590	-0.2137	1.4

The results of numerical calculations to estimate the optimal values of the relaxation parameter are shown in the Table 2.3. The first and the second columns show the number of grid points in the computational domain. The third

